Online Submissions: wjg.wjgnet.com
wjg@wjgnet.com
doi:10.3748/wjg.14.3693

World J Gastroenterol 2008 June 21; 14(23): 3693-3709
World Journal of Gastroenterology ISSN 1007-9327

BASIC RESEARCH

Negundoside, an iridiod glycoside from leaves of *Vitex negundo*, protects human liver cells against calcium-mediated toxicity induced by carbon tetrachloride

Sheikh A Tasduq, Peerzada J Kaiser, Bishan D Gupta, Vijay K Gupta, Rakesh K Johri

Sheikh A Tasduq, Peerzada J Kaiser, Bishan D Gupta, Vijay K Gupta, Rakesh K Johri, Indian Institute of Integrative Medicine, CSIR, Jammu-Tawi-180001, Jammu and Kashmir, India

Author contributions: Tasduq SA designed the study, performed the experiments, analyzed the data, drafted the manuscript and contributed in use of new reagents/analytic tools; Kaiser PS was equally responsible as the first author for performing the experiments and helping in data setting, statistics, arrangement of figures and manuscript drafting; Gupta BD performed the chemistry experiments; Gupta VK worked on the data analysis, application of statistics and manuscript correction; Johri RK was the group leader and was responsible for checking the hypothesis of research study and final corrections of the manuscript and acquired funding for the study.

Supported by Indian Institute of Integrative Medicine, Council of Scientific and Industrial Research

Correspondence to: Sheikh A Tasduq, PhD, Scientist, Experimental Toxicology Lab, Division of Pharmacology, Indian Institute of Integrative Medicine, CSIR, Canal Road, Jammu 180001, Jammu and Kashmir, India. tasduq11@gmail.com
Telephone: +91-191-2569000-10 Fax: +91-191-2569333
Received: December 10, 2007 Revised: April 1, 2008
Accepted: April 8, 2008
Published online: June 21, 2008

Abstract

AIM: To evaluate the protective effect of 2'-p-hydroxy benzoylmussaenosidic acid [negundoside (NG), against carbon tetrachloride (CCl_4)-induced toxicity in HuH-7 cells.

METHODS: CCl_4 is a well characterized hepatotoxin, and inducer of cytochrome P450 2E1 (CYP2E1)-mediated oxidative stress. In addition, lipid peroxidation and accumulation of intracellular calcium are important steps in the pathway involved in CCl_4 toxicity. Liver cells (HuH-7) were treated with CCl_4, and the mechanism of the cytoprotective effect of NG was assessed. Silymarin, a known hepatoprotective drug, was used as control.

RESULTS: NG protected HuH-7 cells against CCl_4 toxicity and loss of viability without modulating CYP2E1 activity. Prevention of CCl_4 toxicity was associated with a reduction in oxidative damage as reflected by decreased generation of reactive oxygen species (ROS), a decrease in lipid peroxidation and accumulation of intracellular Ca^{2+} levels and maintenance of intracellular glutathione homeostasis. Decreased mitochondrial membrane potential (MMP), induction of caspases mediated DNA fragmentation and cell cycle arrest, as a result of CCl_4 treatment, were also blocked by NG. The protection afforded by NG seemed to be mediated by activation of cyclic adenosine monophosphate (cAMP) synthesis and inhibition of phospholipases (cPLA2).

CONCLUSION: NG exerts a protective effect on CYP2E1-dependent CCl_4 toxicity *via* inhibition of lipid peroxidation, followed by an improved intracellular calcium homeostasis and inhibition of Ca^{2+}-dependent proteases.

Key words: Negundoside; Silymarin; HuH-7; Carbon tetrachloride; CYP 2E1; Oxidative stress; Calcium; Toxicity

Peer reviewers: Kunissery A Balasubramanian, Professor, Christian Medical College, Gastrointestinal Sciences, Ida Scudder Road, Vellore 632004, India; Hitoshi Togashi, Associate Professor, Department of Gastroenterology, Course of Internal Medicine and Therapeutics, Yamagata University School of Medicine, 2-2-2 Iida-Nishi, Yamagata 990-9585, Japan

Tasduq SA, Kaiser PJ, Gupta BD, Gupta VK, Johri RK. Negundoside, an iridiod glycoside from leaves of *Vitex negundo*, protects human liver cells against calcium-mediated toxicity induced by carbon tetrachloride. *World J Gastroenterol* 2008; 14(23): 3693-3709 Available from: URL: http://www.wjgnet.com/1007-9327/14/3693.asp DOI: http://dx.doi.org/10.3748/wjg.14.3693

INTRODUCTION

Natural products from plant sources have extensive past and present use in treatment of diverse diseases and serve as compounds of interest both in their natural form and as templates for synthetic modification. The importance of natural products in modern medicine has been well recognized. More than 20 new drugs, launched world over between 2000 and 2005, originate from natural products. Scrutiny of medical indications by source of compounds has demonstrated that natural products and related drugs are used to treat 87% of all categorized human diseases (infectious and non-

infectious)[1].

Vitex negundo (verbenaceae) is an important source of such natural drugs. It is a reputed medicinal herb and its parts have been employed as a traditional cure in Asian systems of medicine (Indian, Chinese, Malaysian) for a variety of disease conditions. A number of pharmacological activities have been attributed to *V. negundo*, such as: analgesic and anti-inflammatory activity[2], enzymes inhibition[3], nitric oxide scavenging activity[4], snake venom neutralization activity[5], antifeeding activity[6], antiradical and antilipoperoxidative[7], CNS activity[8], hepatoprotective activity[9], anti-bacterial activity[10], anti-fungal[11], larvicidal activity [12], antiandrogenic effects[13], mosquito repellent activity[14].

In the recent past, some of our work and work as reported by others on botanical products from *V. negundo* have shown a promising hepatoprotective activity[9,15]. This activity has been evaluated against various hepatotoxic agents including carbon tetrachloride (CCl_4). CCl_4 is a well established and widely used hepatotoxin and the principle cause of CCl_4-induced liver injury is proposed to be lipid peroxidation by free radical derivatives of CCl_4. CCl_4 is activated by NADH-CYP 450 2E1 system of the liver endoplasmic reticulum and converted into trimethyl CCl_3 radicals (*via* reductive dehalogenation) and, under aerobic conditions, in the more reactive trichloromethyl peroxy radical CCl_3OO^*. Formation of the radicals CCl_3^* and CCl_3OO^* causes oxidative stress. The CYP 2E1-mediated metabolism results in generation of reactive oxygen species, which further contributes to the development of cellular injury[16]. Also, considerable evidence suggests that CCl_4 modifies the expression levels of several pro-apoptotic and anti-apoptotic growth factors and receptors[17] especially during chronic administration. CCl_4 has been shown to be a carcinogen and has been classified as a group 2B carcinogen by inducing gene conversion, homozygosity and intra-chromosomal recombinations[18].

It was, therefore, our interest to investigate, in-depth, the mechanism of modulation of CCl_4-induced toxic manifestations with 2'-p-hydroxybenzoylmussaenosidic acid [negundoside (NG)] (a purified irridoid glycoside from leaves of *Vitex negundo*), particularly inhibition of downstream CYP 2E1 cascade of pro-apoptotic events with reference to the following: (1) role of CYP 450 2E1 activation on calcium-mediated oxidative stress; (2) involvement of calcium in phospholipase A2 (PLA2) and cyclic adenosine monophosphate (cAMP) regulation; (3) effect of activated cPLA2 on mitochondrial depolarization, inducing cytochrome C release resulting in caspase mediated apoptosis.

MATERIALS AND METHODS

Chemicals

DMEM F12 medium, Fetal calf serum, trypsin-EDTA solution, 2', 7'-dichlorofluoresceine diacetate (DCF-DA), rhodamine-123 (Rh-123), propidium iodide (PI), DNase-free RNase, proteinase K, 3-(4,5-dimethylthiazole-2-yl)-2,5-diphenyltetrazolium bromide (MTT), Hoechst 33258, cyclosporine A, penicillin, streptomycin, L-glutamine, pyruvic acid, camptothecin, malondialdehyde (MDA) and other biochemicals were purchased from Sigma Chemicals Co. (St. Louis, Mo). Caspase-3 (ApoAlert caspases assay kits) were from B.D. Clontech, USA. Phospholipase A2 (PLA2) and cyclic adenosine triphosphatase (cAMP) were measured by commercially available kits from Cyman company, USA, and R&D systems, USA respectively. Protein concentration was measured using the BCA Protein Assay Kit from Pierce (Rockford, IL, USA).

Collection and identification of test material

Aerial parts of the plant *Vitex negundo* Linn were collected locally during August to October. Plant material was identified and authenticated by examination of the morphological characteristics by taxonomist of the Institute. A voucher specimen has been deposited in Indian Institute of Integrative Medicine (I.I.I.M.) Jammu Herbarium under collection No. 17814.

Extraction procedure for preparation of NG

The shade dried and powdered leaves (1 kg) of *V. negundo* were soaked in ethanol (5 L) and kept overnight. The percolate was filtered and concentrated under reduced pressure at below 50℃. The extraction procedure was repeated three times more using 3 L of ethanol each time. The combined ethanol extract was stirred with water (300 mL) for 1 h and filtered through Celite. The aqueous extract was concentrated at 50℃ and finally dried in vacuum desiccators.

Isolation of NG

The ethanol extract (50 g) of *V. negungo* was adsorbed over silica gel (100 g) to make slurry which was packed over a column of silica gel (1 kg) packed in chloroform. Elution was done with chloroform followed by mixture of chloroform and methanol. Elution with 10% methanol in chloroform gave agnuside followed by mixture of agnuside and negundoside and then negundoside. The compounds were characterized on the basis of ^{1}HNMR, ^{13}CNMR mass spectral data (data not shown) and standardized by HPLC (Figure 1).

Cell culture

The study was carried out using as a model a human hepatoma HuH-7 cells line (ATCC-USA), a generous gift from Dr. Vijai Kumar, International Centre for Genetic Engineering and Biotechnology (ICGEB), New Delhi, India. Cells were grown in Dulbecco's Modified Eagle's Medium (DMEM) containing 10% fetal calf serum (FCS), supplemented with 100 Units/mL penicillin, 100 mg/L streptomycin in a humidified atmosphere in 5% CO_2 at 37℃, and were sub-cultured at 1:5 ratio once a week.

Cell treatment

FCS was reduced to 3% for the experiments. Cells were plated at a density of 3×10^4 cells/cm^2 and maintained in culture medium for 12 h. Stock solutions of CCl_4, NG and silymarin were prepared fresh to avoid

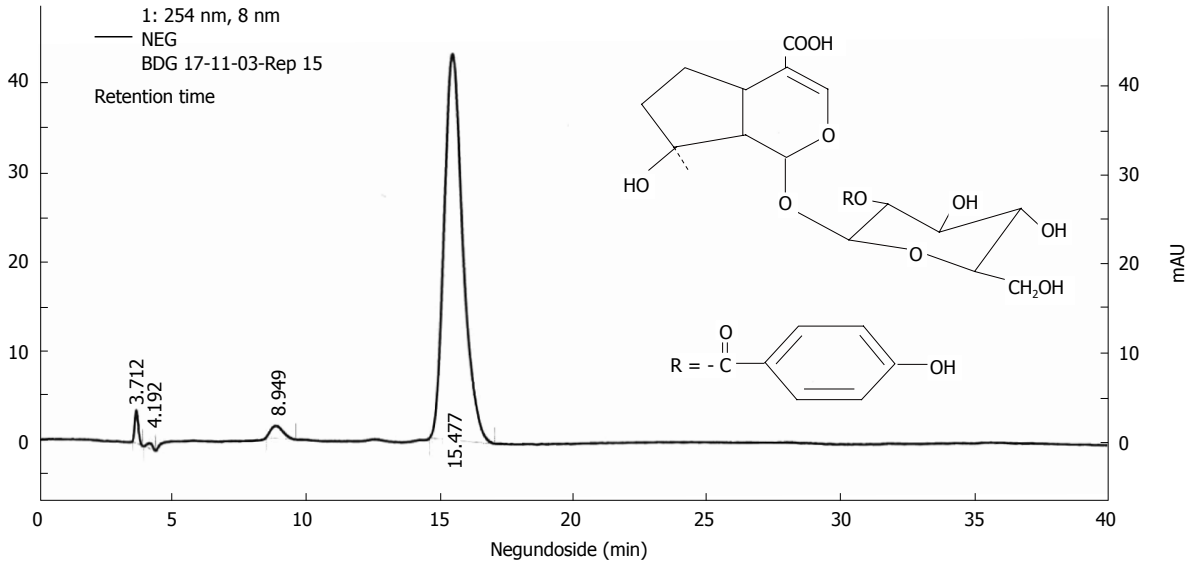

Figure 1 Finger print profile and chemical structure of NG. The HPLC profile of NG was performed by employing Shimadzu HPLC system consisting of a diode array detector and C18 column (5 μm, 250 mm x 4.0 mm I.D.) by UV detection at 254 nm. NG was resolved on a mobile phase consisting of methanol: 2% acetonitrile (30:70) and delivered at a flow rate of 0.6 mL/min. The chromatogram is representative of one of three independent analyses.

oxidation. For CCl_4 toxicity experiments, test substances, were added to the cell cultures an hour prior to CCl_4 treatment. Cells or supernatant were then collected for determination of various parameters.

Cytotoxicity assays

Cells were seeded onto 24-well plates, and after the corresponding treatment, the medium was removed and cell viability was evaluated by assaying for the ability of functional mitochondria to catalyze the reduction of MTT to form formazan salt by mitochondrial dehydrogenases, as described[19] and determined by ELISA reader at 565 nm (Multiskan Spectrum; Thermo Electron Corporation, USA).

Cellular and nuclear morphology

The cellular and nuclear morphology was observed under the light microscope (Nikon Eclipse TE2000U), at 40 × magnification, or under fluorescent microscopy, using Hoechst 33258 staining method as described[20] with certain modifications. Briefly, untreated and treated HuH-7 cells in 6 well plates were harvested by trypsinization, centrifuged at 100 × *g* for 5 min and washed twice with PBS. Cells were gently suspended in 100 μL PBS and fixed in 400 μL cold acetic acid: methanol (v/v = 1:3) overnight at 4℃. Cells were washed again in 1 mL of fixing solution, suspended in the residual volume of about 50 μL, spread on a clean slide and dried overnight at room temperature. One milliliter of staining solution (Hoechst 33258, 10 mg/L in 0.01 mol/L citric acid and 0.45 mol/L disodium phosphate containing 0.05% Tween 20) was poured on each slide and stained for 30 min under subdued light at room temperature. Slides were washed under gentle flow of tap water, rinsed in distilled water followed by in PBS. While wet, 50 μL of mounting fluid (PBS:glycerol, 1:1) was poured over the center of slide and covered with glass cover slip. The slides were sealed with nail polish and observed for any nuclear morphological alterations and apoptotic bodies under inverted fluorescence microscope (Nikon Eclipse TE2000U, magnification 40X) using UV excitation.

Anti-hemolytic activity

Anti-hemolytic activity of NG and silymarin was studied as described[21]. Briefly, blood was collected from healthy volunteers and centrifuged (3000 r/min) with an equal volume of sterilized Alsver solution (2% dextrose, 0.8% sodium citrate, 0.05% citric acid, and 0.42% sodium chloride in water) to obtain the packed cells. The cells were washed with isosaline (0.85%, pH 7.4) and diluted with phosphate buffer (0.15 mol/L, pH 7.4). RBCs (10^8 cells/mL) were incubated with triton × 100 (1 g/L) to induce 100% cell lysis, in absence and presence of test materials at 37℃ for 1 h. The *A* of the supernatant was determined at 540 nm.

CYP2E1 catalytic activity assay

CYP2E1 activity was determined by assaying *P*-nitrophenol hydroxylation in rat liver microsomes prepared by calcium precipitation method as described earlier[22]. In brief, 1 mg microsomes in presence and absence of test material caused hydroxylation of 100 mmol/L aniline hydrochloride in presence of 30 mmol/L cumene hydroperoxide in 0.1 mol/L Tris buffer, pH 7.5. Liberated *p*-aminophenol was treated with 1 mL of 1 mol/L Na_2CO_3 and 1 mL of 2% phenol solution in 0.5 mol/L NaOH. The samples were allowed to stand at room temperature for 30 min and read at 630 nm.

Lipid peroxidation analysis

Cells were plated onto 60 mm Petri dishes, and at the end of the treatment they were washed twice in cold PBS and harvested using rubber policeman in 1 mL PBS. To the resulting cell suspension, we added 2 mL

of TCA-TBA reagent (15% TCA + 0.375% TBA in 5 mol/L HCl) in glass tubes. Tubes were kept in a boiling water bath (100℃) for 1 h, and then cooled to room temp. The contents were centrifuged at 1500 × *g* for 10 min. Absorbance of the supernatants was read at 535 nm against blank. Malonyldialdehyde (MDA) was used to draw the standard curve. The results were expressed as nmoles MDA/mg protein.

In other set of experiments, 1 g/L of rat liver microsomes in 0.15 mol/L NaCl were incubated with 0.1 mmol/L $FeSO_4$ and 35 mmol/L H_2O_2 in the presence and absence of test materials to stimulate lipid peroxidation. Generation of MDA was determined by assaying for thiobarbituric acid-reactive substances (TBARS) as described[22].

Determination of glutathione levels

Cells were seeded onto 60 mm Petri dishes and collected after the corresponding treatments. The total GSH content (reduced form) of samples was assayed as described[23]. Briefly, after treatments, cells were washed with ice cold PBS containing 10 mmol/L EDTA and centrifuged at 1500 × *g*. The cell pellets were resuspended in PBS/EDTA solution with 35% perchloric acid. The cell suspensions were kept on ice for 10 min and vortexed in between 5 times. Cell suspension was centrifuged at 13000 r/min for 10 min at 4℃. The supernatant was transferred to fresh tubes and the pH adjusted to 7 with triethanolamine, 1 mol/L, K_2CO_3 1.65 mol/L and EDTA 30 mmol/L. The contents were centrifuged at 13000 r/min for 10 min. To the 50 μL of the supernatant, we added 1850 μL of PBS/EDTA solution and 100 μL of o-phthaldehyde (1 g/L in methanol). The samples were incubated in the dark for 20 min and read at 350 nm (excitation) and 420 nm (emission) with a fluorescent spectrofluorometer (Perkin Elmer; LS-55).

Determination of cytochrome C by HPLC

Cytochrome C was determined as described[24]. Briefly, the reaction medium (2.5 mL) containing mitochondria (1 mg protein/mL) was 0.2 mol/L sucrose, 1 mmol/L KH_2PO_4, 5 mmol/L succinate, 2 μmol/L rotenone, 10 mmol/L Tris-MOPS, pH 7.3 at 25℃. Mitochondria were preincubated with test materials [NG, silymarin and cyclosporin A (CsA; 0.2 μmol/L)] for 10 min, and then in presence of CCl_4 (2 mmol/L) for 30 min. After incubation, aliquots of mitochondrial suspensions were centrifuged at 11000 × *g* for 8 min to obtain the supernatant. Finally, the supernatant (50 μL) was introduced into an HPLC system equipped with a reverse-phase C4 Cosmosil column (150 mm × 4.6 mm, 5-μm particle size, equipped with a UV-visible detector (393 nm). The column (Spelco; Supercosil LC-304; 24 μm × 4.6 μm × 5 μm) was eluted with a linear gradient of acetonitrile-water (solvents modified with 0.1 mL/L trifluoroacetic acid); the gradient started at 20% acetonitrile and changed to 60% during 12 min and the flow rate was 1.0 mL/min. The column was then washed with the 60% acetonitrile for 5 min followed by reequilibration for 5 min in the 20% acetonitrile.

Preparation of rat liver mitochondria

Mitochondria from livers of rats (Wistar) were prepared as described[25]. In brief, rat livers were washed once with physiological saline, dissected and washed twice in cold isolation solution (200 mmol/L D-mannitol, 70 mmol/L sucrose, 2 mmol/L HEPES, 0.5 g/L BSA). Dissected livers were minced with two volumes of isolation solution and homogenized (IKA homogenizer-WERK, Ultra Turrax, T 25 B). The homogenate was diluted with 7 volumes of isolation buffer and centrifuged for 10 min at 560 × *g*. The supernatant collected was again centrifuged for 15 min at 7000 × *g*. The mitochondrial pellet was collected and resuspended in 2.5 volumes of isolation solution and stored at -80℃ until use.

Measurement of intracellular calcium

Intracellular calcium levels were determined with the fluorescent calcium indicator fura2-AM by ratiometric fluorimetry as described[26]. HuH-7 cells were detached from the plate using HBSS buffer (118 mmol/L NaCl, 4.6 mmol/L KCl, 10 mmol/L glucose, 20 mmol/L Hepes, pH 7.2) containing 0.02% EDTA, resuspended in HBSS with 1 mmol/L $CaCl_2$, and incubated with 1 μmol/L fura2-AM in the dark for 1 h at 37℃. Cells were washed with HBSS/$CaCl_2$, and resuspended in HBSS/$CaCl_2$ at a density of 1×10^6 cells/mL. EGTA (10 mmol/L) was added at the beginning of the experiment, followed by a 60 s-equilibration period[27]. Intracellular free calcium measurements were performed at 37℃ using a ratiometric fluorescence spectrophotometer (Perkin-Elmer LS 50B). Intracellular Ca^{2+} concentration was estimated as described[28] based on the equation: $[Ca^{2+}]_i = K_d[(R-R_{min})/(R_{max}-R)]F_{min(380)}/F_{max(380)}$, where R is F_{340}/F_{380} ratio, R_{min} and R_{max} are the ratios with 50 mmol/L digitonin, and 50 mmol/L digitonin + 11 mmol/L $CaCl_2$, respectively. K_d represents the apparent dissociation constant of Fura-2 (224 nmol/L) and $F_{min(380)}/F_{max(380)}$ are the fluorescence values of digitonized cells without or with 11 mmol/L $CaCl_2$, respectively.

Flow cytometric analysis of mitochondrial membrane potential ($\Delta\psi_m$)

Changes in the mitochondrial membrane potential ($\Delta\psi_m$) were examined by monitoring the cell fluorescence after staining with rhodamine 123 (Rh123) as described[29]. Rh123 is a membrane permeable fluorescent cationic dye that is selectively taken up by mitochondria directly proportional to the MMP[30]. The intensities from Rh123 and PI were determined using a BD-LSR flow cytometer equipped with electronic doublet discriminating capability.

Intracellular measurement of reactive oxygen species (ROS)

The production of ROS was monitored with DCF-DA as the probe[31]. DCF-DA diffuses through the cell membrane and is enzymatically hydrolyzed by

intracellular esterases to nonfluorescent DCF-H, which is then rapidly oxidized to the highly fluorescent DCF in presence of ROS. Treated and non-treated HuH-7 cells were incubated for 1 h with DCF-DA (2 μmol/L) and, after the washing of cells, the production of free radicals were assessed *in situ* as the enhancement of fluorescence at excitation wavelength of 500 nm and emission wavelength of 520 nm and was measured in a fluorescent plate reader (Perkin Elmer LS 55, USA).

Measurement of intracellular H_2O_2

Intracellular H_2O_2 levels were analyzed using 123 dihydrorhodamine (123-DHR) as specific fluorescent dye probe as described by Katiyar *et al* with modifications for HuH-7 cells[32]. Briefly, non-treated and treated HuH-7 were washed twice with PBS and incubated in the culture medium without FCS and loaded with 123-DHR (5 μmol/L). Cells were further incubated for 45 min to irreversibly oxidize and convert DHR to fluorescent compound rhodamine 123 and fluorescence was read with aid of spectrofluorometer (Perkin Elmer LS 55, USA) with excitation wavelength 485 nm and emission wavelength of 530 nm. The cells for fluorescent-based assays were grown onto sterile black fluorescent plates (96 well format; Nunc, Denmark).

Cell cycle analysis (apoptosis)

Cell cycle was analysed as described by Yang *et al*[33]. Briefly, non-treated and treated HuH-7 cells were harvested by trypsinization, centrifuged at 1500 × *g* for 5 min, washed with PBS, and fixed in 70% ethanol at 4℃ overnight. Fixed cells were washed twice with PBS and incubated in PBS containing 1.5 mg/L RNase A for 1 h at 37℃, followed by staining with 5 μL PI (1 mmol/L stock) for 20 min on ice. The cells were analyzed for DNA content using BD-LSR flow cytometer equipped with electronic doublet discrimination capability using blue (488 nm) excitation from argon laser. Data were collected in list mode on 10 000 events for FL2-A *vs* FL2-W.

DNA laddering

DNA fragmentation was analysed as described by Yang *et al*[33]. Briefly, HuH-7 cells treated or untreated were harvested and centrifuged at 1500 × *g* for 5 min. After washing twice with PBS/ethylenediamine-*N, N, N′, N′*-tetraacetic acid (EDTA). Cells were incubated in a lysis buffer [0.5 mL/L Triton X-100, 10 mmol/L EDTA, 0.4 g/L proteinase K, and 10 mmol/L Tris-HCl, pH 7.4] at 56℃ for 1 h. Cell lysate was treated with 0.4 g/L RNase at 37℃ for 30 min. The genomic DNAs were purified by phenol/chloroform extraction and ethanol precipitation, and resuspended in a Tris-EDTA buffer, DNA fragments were stained with ethidium bromide and visualized by 2.5% agarose electrophoresis.

Enzymic assay of caspase 3-activity

Caspase activation was measured using a caspase 3 fluorometric assay kit (BD Apoalert caspase 3 fluorescent assay kit). HuH-7 cells, treated or untreated were harvested, and centrifuged (approximately 1 mg protein) at 400 × *g* for 5 min. The cell pellets were re-suspended in 50 μL of chilled cell lysis buffer and incubated on ice for 10 min, and the lysates were centrifuged at 15 000 × *g* for 10 min at 4℃ to precipitate cellular debris. A total of 50 μL of cell lysates was incubated with 50 μL of reaction buffer/DTT mix. DEVD-CHO was used as an inhibitor of caspase 3 in an induced sample. Five μL of 1 mmol/L caspase-3 substrate (DEVD-AFC at a final concentration of 50 μmol/L) was added to each sample. The samples were incubated at 37℃ for 1 h and read on a spectrofluorometer (Perkin Elmer LS 55) with excitation wavelength 400 nm and emission wavelength of 505 nm.

Cytosolic phospholipase A_2 assay

$cPLA_2$ activity was measured in cell lysates, using $cPLA_2$ assay kit (Cayman Chemical Company $cPLA_2$ assay kit) as per the instructions of the supplier. The kit involves the principle that $cPLA_2$ exhibits specificity towards arachidonic acid. Arachiconyl thio-PC is used as a synthetic substrate to detect the phospholipase activity. Hydrolysis of the arachiconoyl thioester bond at the *sn*-2 position by $cPLA_2$ releases free thiol which are detected by DTNB (5, 5'-dithiobis-2-dinitrobenzoic acid).

Adenosine 3', 5'-cyclic monophosphate (cAMP) assay

cAMP activity was measured in the cell lysates, using cAMP assay kit (R&D Systems, Inc, cAMP assay kit) as per the instructions of the supplier. The kit is based on the competitive binding technique in which cAMP present in a sample competes with a fixed amount of horseradish peroxidase (HRP)-labeled cAMP for sites on a mouse monoclonal antibody. During the incubation, the monoclonal antibody becomes bound to the goat anti-mouse antibody coated onto the microplate. Following a wash to remove excess conjugate and unbound sample, a substrate solution is added to the wells to determine the bound activity. The colour developed was stopped and the absorbance read at 450 nm. The intensity of the colour is inversely proportional to the concentration of cAMP in the sample.

2, 2'-azino-di-[3-ethylbenzthiazoline sulphate] oxidation inhibition assay (ABTS assay)

The assay was performed using antioxidant assay kit from Cayman Chemical Company, as per the instructions by the manufacturer. The assay was used to access the ability of the test materials (NG, Silymarin *etc*) to inhibit the oxidation of ABTS to $ABTS^{\cdot+}$ by metmyoglobin. The amount of $ABTS^{\cdot+}$ produced in absence and presence of test material was monitored by reading absorbance at 750 nm. Suppression of the absorbance at 750 nm in presence of test material is proportional to their antioxidant activity. The capacity of the antioxidant activity (inhibition of $ABTS^{\cdot+}$ formation) in the test sample was compared with that of Trolox, a water-soluble tocopherol analogue.

1,1-diphenyl-2-picrylhydrazyl (DPPH) discolouration assay

This assay was performed as described by Gonzalez

et al[34]. In brief, for the assay, various concentrations of test compound were added to 3 mL of DPPH solution (20 mg/L methanol) and incubated for 5 min at 25℃. The absorbance was measured al 517 nm. A 100% decoloration was established using methanol-water 2:1 and the percentage of DPPH decoloration was calculated.

Superoxide anion scavenging activity

In vitro effect of NG on superoxide anion radical generation was studied as described previously[35]. Two reaction systems used were: (a) enzymic ; (b) non-enzymic. System (a) comprised of 100 μmol/L xanthine, 600 μmol/L nitroblue tetrazolium (NBT) and 0.07 U/mL xanthine oxidase in 50 mmol/L sodium carbonate pH 9.2, incubated for 10 min in presence and absence of test materials and *A* read at 560 nm. System (b) comprised of 10 μmol/L phenazine methosulphate, 78 μmol/L NADH, 25 μmol/L NBT, incubated for 2 min in presence and absence of test materials and *A* read at 560 nm.

Protein estimation

Protein concentration was measured with BCA Protein Assay Kit from Pierce (Rockford, IL, USA) as per the instructions of the manufacturer.

Statistical analysis

Results are expressed as mean ± SD. Comparisons were made between control and treated groups unless otherwise indicated using unpaired Student's *t*-test and *P* values < 0.05 were considered statistically significant.

RESULTS

Standardization of NG

For better scientific and clinical acceptability and proper global positioning of plant based products, it has become implicit to determine their chemical profile data on the basis of purity of compound. In this respect we have developed the HPLC protocol for NG (Figure 1). HPLC profile confirmed that NG was isolated as < 95% pure.

Cytoprotective and membrane stabilizing effect of NG and silymarin against CCl_4-induced cytotoxicity in HuH-7 cells

CCl_4 produced a concentration dependent loss of viability in HuH-7 cells as evaluated by MTT assay. At 24 h of incubation, the IC50 value of CCl_4 was found to be 2 mmol/L approximately (1.958 mmol/L; Figure 2A). This concentration was used to generate oxidative stress to study the cytoprotective effect of NG and silymarin in further experimentations. NG alone was not toxic under the assay conditions up to a concentration of 400 mg/L. However, silymarin at concentrations above 50 mg/L produced loss of cell viability, with an estimated IC50 value of 413.38 mg/L (Figure 2B).

To characterize the protective effect of NG and silymarin on CCl_4 induced cytotoxicity in HuH-7 cells,

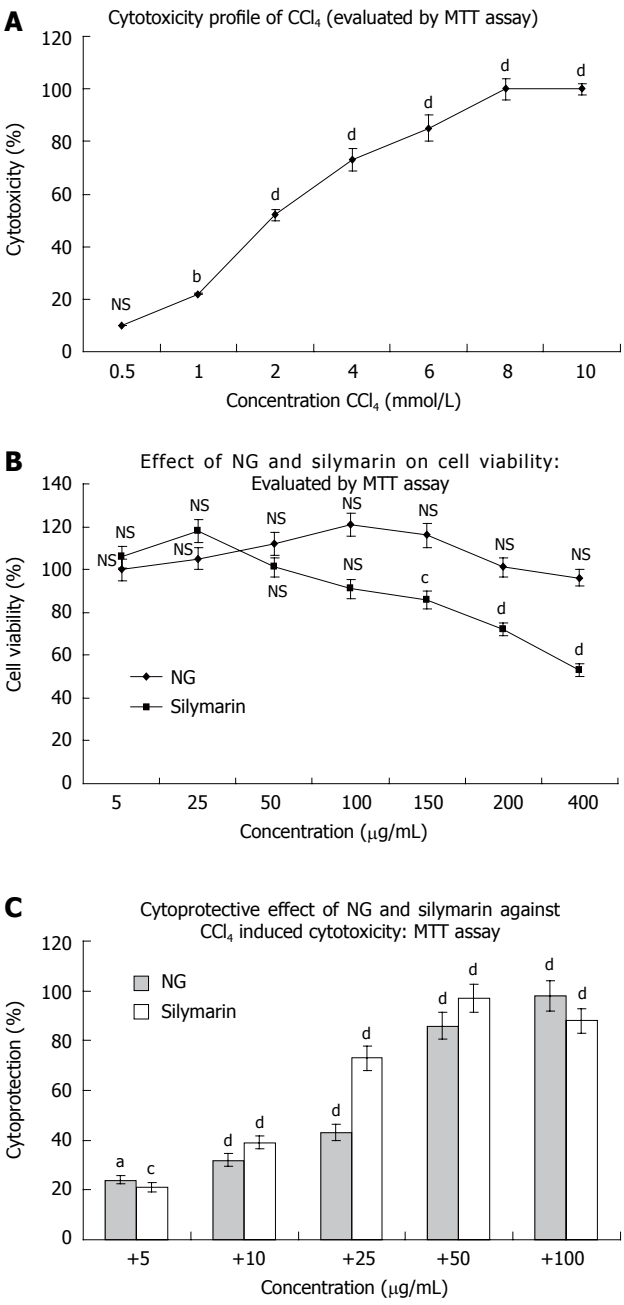

Figure 2 Cytotoxicity profile of CCl_4 and protective effect of NG and silymarin on CCl_4-induced inhibition of cellular proliferation in HuH-7 cells. For cell proliferation assay, HuH-7 cells grown in 24-well culture plate were incubated with indicated concentrations of test materials. Cell proliferation was assessed by MTT reduction assay. **A**, **B**: Represents inhibition of cell proliferation by CCl_4 and test materials (NG and silymarin); **C**: Represents protection of NG and silymarin, against CCl_4 induced inhibition of cell proliferation. HuH-7 cells were treated with various concentrations of NG and silymarin (5 to 100 mg/L) 1 h before treatment with CCl_4 for 24 h and the cell proliferation was determined by MTT reduction assay. Control wells received medium containing DMSO (< 0.2 mL/L). The % cell cytoxicity, % viability and % cytoprotection was calculated as, % Cytotoxicity = (Control - Test)/Control x 100, % Cell viability = % Cytotoxicity - 100, % Cytoprotection = 100 - (Treated - Control)/(CCl_4 - Control) x 100. Data are mean ± SD (n = 8) and representative of one of three similar experiments and statistically significant *P* values: $^bP < 0.01$; $^dP < 0.001$; $^aP < 0.02$; $^cP < 0.05$; NS: Non-significant, CCl_4 treated *vs* control cells; CCl_4 + LIV-1/silymarin *vs* CCl_4 treated cells.

dose-response experiments were conducted using various concentrations of NG and silymarin. NG showed a significant dose dependent protective effect

against CCl_4 induced loss of cell viability. The PC50 (50% protective concentration) for NG was estimated to be 24.46 mg/L and 15.30 mg/L for silymarin (Figure 2C).

Results obtained from MTT assay were in total correlation with the extent of cell death as confirmed by morphological changes observed under light microscope and Hoechst 33258 staining under fluorescence microscopy (Figure 3). Treatment with CCl_4 caused HuH-7 cells to lose their normal structure with signs of cell swelling, most of the cells were detached and monolayer was disturbed (Figure 3 I A compared with Figure 3 I B). These structural changes were prevented to a large extent by 30 and 100 μg/mL of NG and were comparable with the protection offered by silymarin at 50 mg/L (Figure 3 I C-F).

Nuclei of untreated HuH-7 cells appeared prominently round in shape (Figure 3 II A). After exposure with CCl_4, cells showed morphological alterations and condensation of nuclei (Figure 3 II B). The prominent changes were accompanied by an increase in apoptotic bodies and increase in cellular debris. All these alterations were prevented by co-exposure with NG and silymarin in a dose dependent manner (Figure 3 II C-E).

The above mentioned cytoprotective results were further correlated with the membrane stabilizing effect of NG and silymarin against Triton X 100 (1 g/L)-induced membrane disruption in human RBCs. NG showed an effect in the range of 4% to 91% in a concentration dependent manner (5 mg/L to 100 mg/L) against a protective effect of 6% to 88% at the same concentration, shown by silymarin (Figure 4).

Effect of NG and silymarin on CYP2E1 catalytic activity

To study the mechanism by which NG was preventing CCl_4-induced toxicity in HuH-7 cells, the possible interference of NG and silymarin on CYP2E1 activity (aniline hydroxylation) was studied. Hepatic microsomes from Wistar rats were used as a source to assay *in vitro* effect of NG and silymarin on CYP2E1 levels (Figure 5A). In another set of experiments, the CYP2E1 protein levels were analyzed to assay the protective effect of NG and silymarin against oxidation of 2.5 mmol/L ethanol (Figure 5B).

NG alone showed no significant effect on aniline hydroxylation levels at any concentrations used (5 to 100 mg/L), whereas silymarin produced an inhibitory effect in the range of 2.6% to 26.2% at the same concentrations (Figure 5A). Isoniazid (used as a positive control for inhibition of CYP2E1) showed a dose dependent inhibition, with IC50 at 500 μmol/L (data not shown).

Treatment of microsomes with 2.5 mmol/L ethanol caused an increase of 63% in aniline hydroxylation levels. Co-treatment of NG with ethanol showed no inhibitory effect on aniline hydroxylation levels induced by ethanol. However, silymarin caused inhibitions of 8.4%, 41%, 76% and 149% at 10 mg/L, 25 mg/L, 50 mg/L and 100 mg/L, respectively in aniline hydroxylation levels compared to microsomes treated with ethanol alone (Figure 5B).

The results (Figure 5 A and B) show that NG did not inhibit CYP2E21 activity, suggesting that NG is most probably acting as an antioxidant, and not as a CYP2E1 inhibitor and silymarin acts both as an antioxidant, and an inhibitor of CYP2E1.

Effect of NG and silymarin on $FeSO_4$ + H_2O_2 stimulated lipid peroxidation (LPO) in rat liver microsomes and on CCl_4 induced LPO in HuH-7 cells

$FeSO_4$ + H_2O_2 increased LPO in rat liver microsomes by 6.8-fold. Incubation with NG (10 to 100 mg/L) decreased in a range of 3% to 69%, this increase in LPO levels (Figure 6A). Silymarin at the equivalent concentrations showed an enhanced inhibitory effect of 21% to 111%. Treatment of HuH-7 cells with CCl_4, increased LPO levels up to 4.6-fold. NG offered a protective effect against this increase by 10.4%, 21%, 39%, 54% and 131% at 5 mg/L, 10 mg/L, 25 mg/L, 50 mg/L and 100 mg/L, respectively. At similar concentrations, silymarin produced respective inhibitory effects of 17%, 32%, 64%, 146% and 164% (Figure 6B).

Effect of NG and silymarin on the ROS generation induced by CCl_4

Oxidative stress was studied by fluorescence spectrophotometrical analysis of the levels of ROS, using DCF-DA and DHR as the probes. Figure 7 shows the mean values of DCF and DHR fluorescence for cell populations with various treatments. Treatment with CCl_4, increased by 2.1 (DCF) and 2.2-fold (DHR) the production of ROS in HuH-7 cells in comparison with no addition control. NG and silymarin (10 to 100 mg/L) reduced the increase in the ROS levels produced by CCl_4 in a significant and dose dependent manner. NG at 10 mg/L decreased DCF fluorescence intensity by 32% and DHR by 52%. At 50 mg/L, DCF and DHR intensities were decreased by 76% and 105%, respectively. At 100 mg/L, both the fluorescence intensities were down by 104% and 143%. H_2O_2 (500 μmol/L) was used as positive control for ROS generation.

Effect of NG and silymarin on intracellular Ca^{2+} and caspase 3 levels induced by CCl_4

Intracellular Ca^{2+} and caspase 3 levels were increased significantly by CCl_4 treatment, which reflects the requirement of Ca^{2+} and caspase 3 in the overall toxicity pathway of CCl_4 (Figures 8 and 9). CCl_4 caused an increase of 4.8-fold in Ca^{2+} and 2.3-fold in caspase 3 levels in HuH-7 cells. This abnormal rise in Ca^{2+} levels were decreased by NG by 15%, 72% and 106% and caspase 3 levels were decreased by 16%, 92% and 139% at 10 mg/L, 50 mg/L and 100 mg/L, respectively. Silymarin also showed a dose dependent inhibitory effect on Ca^{2+} and caspase 3 levels increased by CCl_4. The effect was 28%, 114% and 207% in Ca^{2+} levels at 10 mg/L, 50 mg/L and 100 mg/L, and 34% and 160% in caspase 3 levels at 10 mg/L and 50 mg/L, respectively. However at 100 mg/L, silymarin showed a less significant effect (28% decrease). Thus, silymarin showed a higher Ca^{2+} inhibitory effect compared to NG, but less caspase 3 inhibition at concentrations

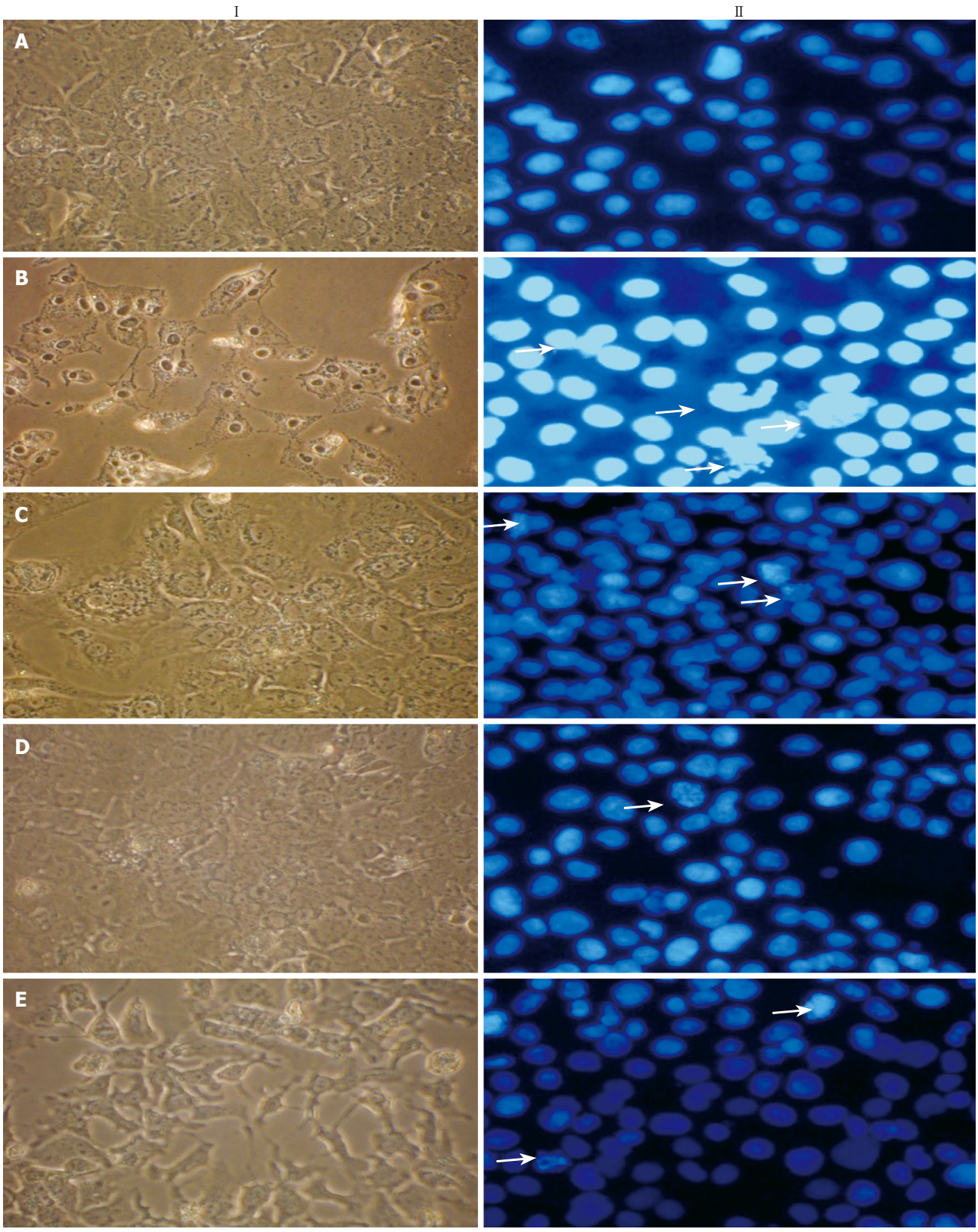

Figure 3 Effect of NG and silymarin against CCl_4-induced altered cellular and nuclear morphology of HuH-7 cells. NG and silymarin rescued CCl_4-induced cellular (Ⅰ) and nuclear morphological (Ⅱ) changes. Cellular morphology was observed by normal phase contrast microscopy, while as nuclear morphology was evaluated by Hoechst 33258 staining of HuH-7 cells and observed under fluorescence microscopy as described in Materials and Methods. These methods detected influences of CCl_4 on cellular and nuclear changes. **A**: Untreated control cells show normal cellular characteristics and rounded nuclei; **B**: Cells treated with CCl_4 (2 mmol/L) for 24 h show altered membrane structure and condensed chromatin/nuclei, apoptotic (arrows) and scattered apoptotic bodies; **C**: Cells incubated with NG (30 mg/L); **D**: Cells incubated with NG (100 mg/L); **E**: Cells incubated with silymarin (50 mg/L), 1 h before the treatment with CCl_4 showed protection against CCl_4-mediated cellular and nuclear alterations.

above 50 mg/L. Cyclosporine (10 μmol/L) was used as positive control for Ca^{2+} inhibition and camptothecin (inducer, 4 μmol/L) and DEVD-CHO (inhibitor, 20 μmol/L) were used as positive controls.

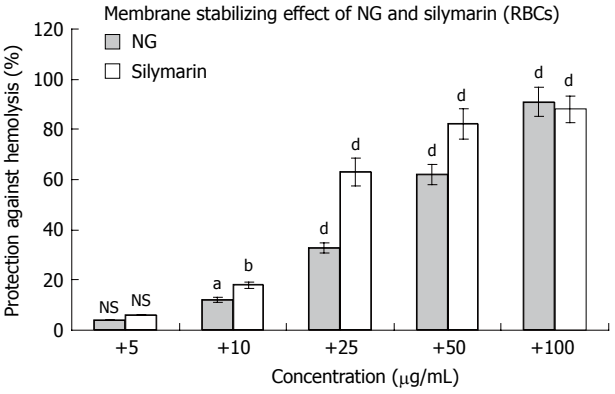

Figure 4 Membrane stabilizing effect of NG and silymarin on human RBCs. RBC suspensions were pre-incubated with or without (control) test materials and triton (1 g/L) in phosphate buffered saline as described in Materials and Methods section. Data are mean ± SD (n = 3) and representative of one of three similar experiments and statistically significant P values: $^{b}P < 0.01$; $^{a}P < 0.05$; $^{d}P < 0.001$; NS = Non-significant. Triton treated *vs* control cells; triton + NG/silymarin *vs* triton treated cells.

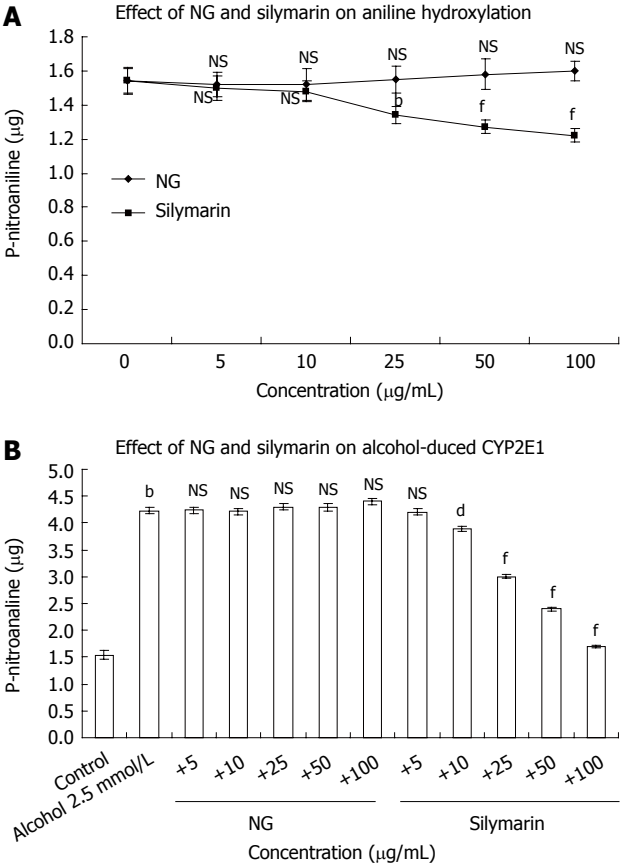

Figure 5 Effect of NG and silymarin *in vitro* on CYP2E1 catalytic activity. **A**: Rat liver microsomes were incubated in the absence or presence of different concentrations (5 to 100 mg/L) of test materials. CYP2E1 activity was assayed by following the hydroxylation of aniline hydrochloride in presence of cumene hydroperoxide as described in Materials and Methods section; **B**: Concentration dependent protection by NG and silymarin against alcohol (2.5 mmol/L)-induced aniline hydroxylase levels in rat liver microsomes. The microsomes were pre-incubated with medium containing various concentrations (5 to 100 mg/L) of test materials for 5 min before addition of alcohol and aniline hydroxylase levels were determined. Data are expressed as mean ± SEM and are from a representative experiments repeated twice and conducted in triplicate. P values: $^{b}P < 0.001$ *vs* the corresponding alcohol-treated microsomes; $^{d}P < 0.001$ and $^{f}P < 0.001$ *vs* alcohol-treated cells in presence of test materials; NS: Non-significant.

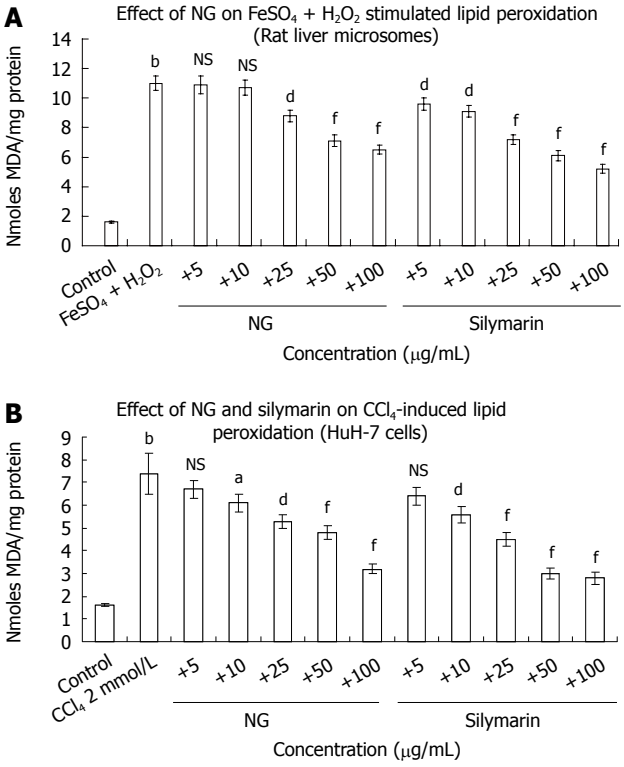

Figure 6 Protective effect of NG and silymarin against stimulated lipid peroxidation. **A**: Anti-lipid peroxidative effect of NG and silymarin *in vitro*. Liver microsomes (1 mg protein/mL, 0.15 mol/L NaCl, pH 7.0) were incubated for 20 min at 37℃ in the absence (control) and presence of 100 mmol/L $FeSO_4$ +/50 mmol/L H_2O_2 (stimulated). In identically set-up Fe^{2+}/H_2O_2-stimulated incubations, NG and silymarin (20 mg/L to 100 mg/L, in 30% DMSO) were added (test C). Control incubations received vehicle only; **B**: HuH-7 cells were pre-incubated for 1 h with medium containing test materials (NG and silymarin) at different concentrations (5 mg/L to 100 mg/L). The cells were further incubated in absence or presence of 2 mmol/L CCl_4 (stimulated) for further 24 h. The cells were harvested by scraping and assayed for the production of MDA using TBARS assay, as described under materials and methods section. Reaction was terminated by the addition of 2.0 mL TCA-TBA reagent (15% TCA, 0.375% TBA in 5mol/L HCl) and LPO content determined as nmol MDA formed/mg protein. Data are expressed as mean ± SD and are from representative experiments repeated twice and conducted in triplicate. Statistical significance, $^{b}P < 0.01$ *vs* the untreated control. $^{d}P < 0.01$; $^{a}P < 0.05$; $^{f}P < 0.001$ and NS: Non-significant *vs* stimulated ($FeSO_4$ + H_2O_2 and CCl_4 treatments).

Effect of NG and silymarin on cytochrome C release from isolated rat liver mitochondria induced by CCl_4

Isolated rat liver mitochondria were used to study the effect of NG and silymarin on cytochrome C release induced by CCl_4 (Figure 10). CCl_4 caused an increase of 2.1-fold in cytochrome C levels, which was inhibited by 75% and 105% at 50 mg/L and 100 mg/L of NG treatment, respectively. Silymarin showed an effect in the range of 27% at 10 mg/L, 135% at 50 mg/L. However at a higher concentration (100 mg/L), silymarin showed a biphasic effect, with a slight increase in cytochrome C levels compared to 50 mg/L (36% increase). Cyclospo-rine 5 μmol/L was used as a positive control for cytochrome C inhibition.

Effect of NG and silymarin on mitochondrial membrane permeability transition onset by CCl_4 in HuH-7 cells

Oxidative damage to mitochondria and the onset of MMP transition seems to play an important role in CCl_4-

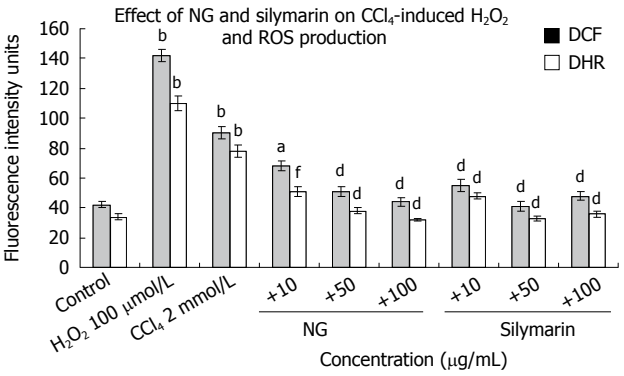

Figure 7 Effect of NG and silymarin on CCl_4-induced ROS production. HuH-7 cells were pre-incubated for 1 h with medium containing test materials (NG and silymarin) at different concentrations (10 to 100 mg/L). The cells were kept for further incubation in absence or presence of 2 mmol/L CCl_4 (stimulated). After 24 h of incubation maintaining the specific treatments, the cells were incubated with serum-free medium containing DCF-DA and 123-DHR and ROS levels were studied as mentioned in material and methods section. H_2O_2 (100 μmol/L) was used as positive control for ROS generation. Data are expressed as mean ± SD and are from representative experiments repeated twice and conducted in triplicate. Statistical significance, $^bP < 0.001$ *vs* the untreated control; $^dP < 0.001$, $^aP < 0.05$; $^fP < 0.01$ *vs* CCl_4-treated cells.

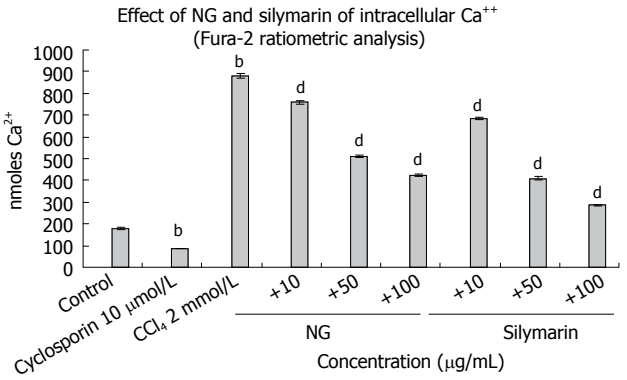

Figure 8 Effect of NG and silymarin against CCl_4-induced cytosolic free Ca^{2+} concentrations. HuH-7 cells pre-incubated for 1 h with medium containing test materials (NG and silymarin) at different concentrations (10 to 100 mg/L) were exposed to CCl_4 (2 mmol/L) for indicated time period, washed and loaded with Fura-2 AM as described in materials and methods section. Cyclosporine (10 μmol/L) was used as positive control. Data are expressed as mean ± SD, and are from a representative experiments repeated twice and conducted in triplicate. Statistical significance: $^bP < 0.001$ *vs* the untreated control, $^dP < 0.001$ *vs* CCl_4 treated cells.

induced toxicity in HuH-7 cells. MMP transitions were analyzed by flow cytometry after staining with Rh123 (Figure 11). Untreated HuH-7 cells were strong in Rh123 fluorescence intensity, suggestive of intact viable cells. A very small percentage of cells (8%) were showing low Rh123 fluorescence, reflective of damaged cells. CCl_4 caused a 6-fold increase in percentage of cells with low Rh123 fluorescence. Incubation in the presence of 50 mg/L and 100 mg/L of NG and silymarin, respectively significantly protected HuH-7 cells from decline in MMP produced by CCl_4.

Effect of NG and silymarin on CCl_4-induced apoptosis in HuH-7 cells

Apoptosis was studied by internucleosomal DNA fragmentation analysis and cell cycle analysis by flow

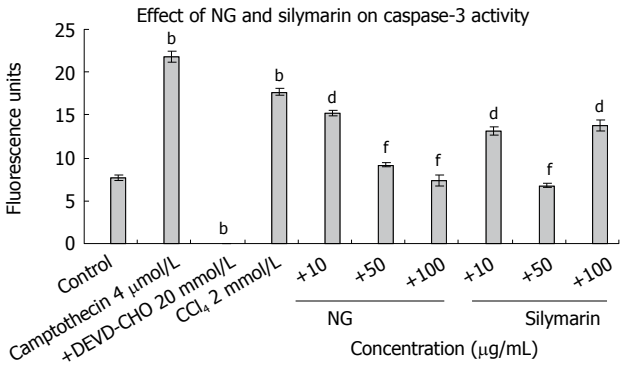

Figure 9 Effect of NG and silymarin against caspase 3-mediated apoptosis. CCl_4 treatment increases caspase 3 activity in HuH-7 cells. HuH-7 cells were treated with CCl_4 in presence or absence of test materials (NG and silymarin) and caspase 3 activity was measured as described in Materials and Methods section. Data are expressed as mean ± SD and are from representative experiments repeated twice and conducted in triplicate. Statistical significance: $^bP < 0.001$ *vs* the untreated control. $^dP < 0.01$; $^fP < 0.001$ *vs* CCl_4-treated cells.

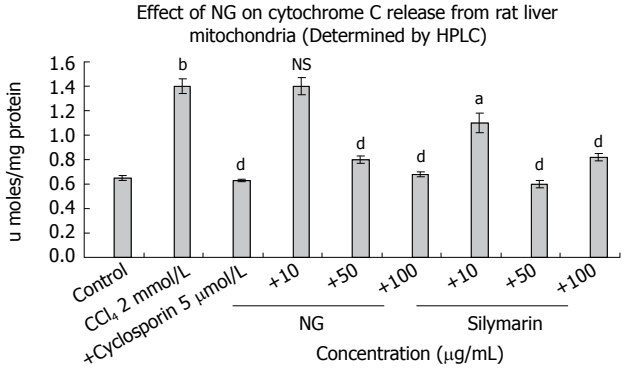

Figure 10 Effect of NG and silymarin against CCl_4-induced cytochrome C release from isolated rat liver mitochondria. CCl_4 treatment causes cytochrome C release form rat liver mitochondria. Mitochondria were treated with CCl_4 in presence or absence of test materials (NG and silymarin) and cytochrome C levels were measured as described in Materials and Methods section. Data are expressed as mean ± SD and are from a representative experiments repeated twice and conducted in triplicate. Statistical significance: $^bP < 0.001$ *vs* the untreated control; $^aP < 0.02$; $^dP < 0.001$ and NS = non-significant *vs* CCl_4 treated mitochondria.

cytometry. A DNA ladder formation was found with cells treated with CCl_4 (Figure 12). Treatment with NG and silymarin protected HuH-7 cells against CCl_4 induced DNA fragmentation.

In cell cycle analysis, treatment with CCl_4 markedly increased proportion of apoptotic cells significantly (49%). NG and silymarin had an obvious anti-apoptosis effect. As shown in Figure 13, the co-treatment with 25 mg/L, 50 mg/L and 100 mg/L of NG markedly reduced the percentage of the apoptotic cells to 27%, 14% and 11%, respectively. Silymarin showed a reduction in apoptotic cells by 21% and 9% at 25 mg/L and 50 mg/L, respectively. At 100 mg/L, however, silymarin had an effect of 18% (Figure 13).

Effect of NG and silymarin on CCl_4-induced alterations in cAMP and $cPLA_2$ levels in HuH-7 cells

To test the effect of CCl_4-induced oxidative stress on cAMP levels in HuH-7 cells, we evaluated cAMP with

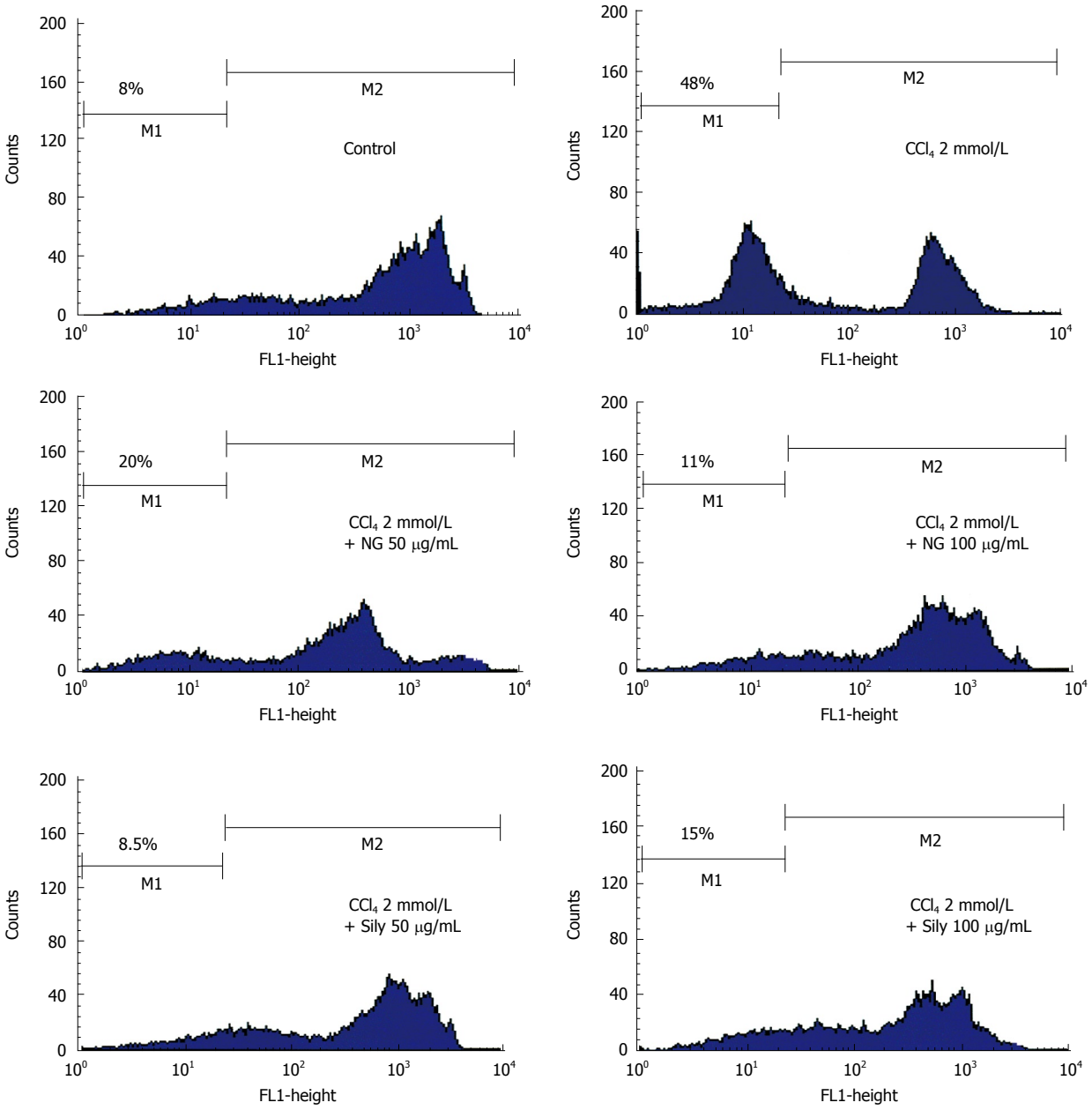

Figure 11 Effect of NG and silymarin against CCl_4-induced loss of mitochondrial membrane potential ($\Delta\psi m$). HuH-7 cells were pre-incubated for 1 h with test materials (NG and silymarin) at mentioned concentrations. The cells were further incubated for 24 h with CCl_4 (2 mmol/L). Thereafter, cells were stained with Rhodamine-123 and analysed by flow cytometry as described in Materials and Methods section. Representative histograms are shown and the percentage of cells in depolarized zone (M1 zone) are shown.

and without CCl_4 and then in the presence of CCl_4 with NG and silymarin. As hypothesized, cAMP levels were significantly reduced by CCl_4. Concomitant treatment of HuH-7 cells with NG significantly increased the levels of cAMP. Similar results were evident with treatment with silymarin. Forskolin (100 μmol/L) was used as a positive inducer of cAMP (Figure 14). On the contrary, phospholipase A2 levels were significantly increased with the CCl_4 treatment (2.3-fold). NG effectively reduced this increase by 44% at 10 mg/L and 304% at 50 mg/L. Silymarin reduced these levels by 97% at 10 mg/L and 136% at 50 mg/L. Bee venom (1 mg/L) was used as positive control to induce cPLA2 levels (Figure 15).

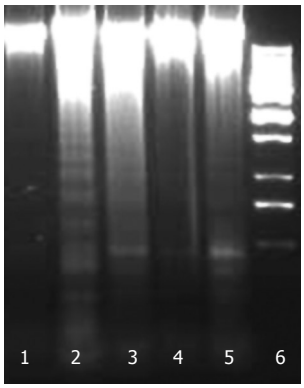

Figure 12 Effect of NG and silymarin against CCl_4-induced DNA fragmentation. HuH-7 cells were pre-incubated for 1 h with test materials (NG and silymarin) at mentioned concentrations. The cells were further incubated for 24 h with CCl_4 (2 mmol/L). Thereafter, genomic DNA was extracted from cells and subjected to gel electrophoresis as mentioned in Materials and Methods section. Lanes: 1: Control; 2: CCl_4 2 mmol/L; 3: CCl_4 2 mmol/L + NG 30 mg/L; 4: CCl_4 2 mmol/L + NG 100 mg/L; 5: CCl_4 2 mmol/L+ Silymarin 50 mg/L; 6: Ladder.

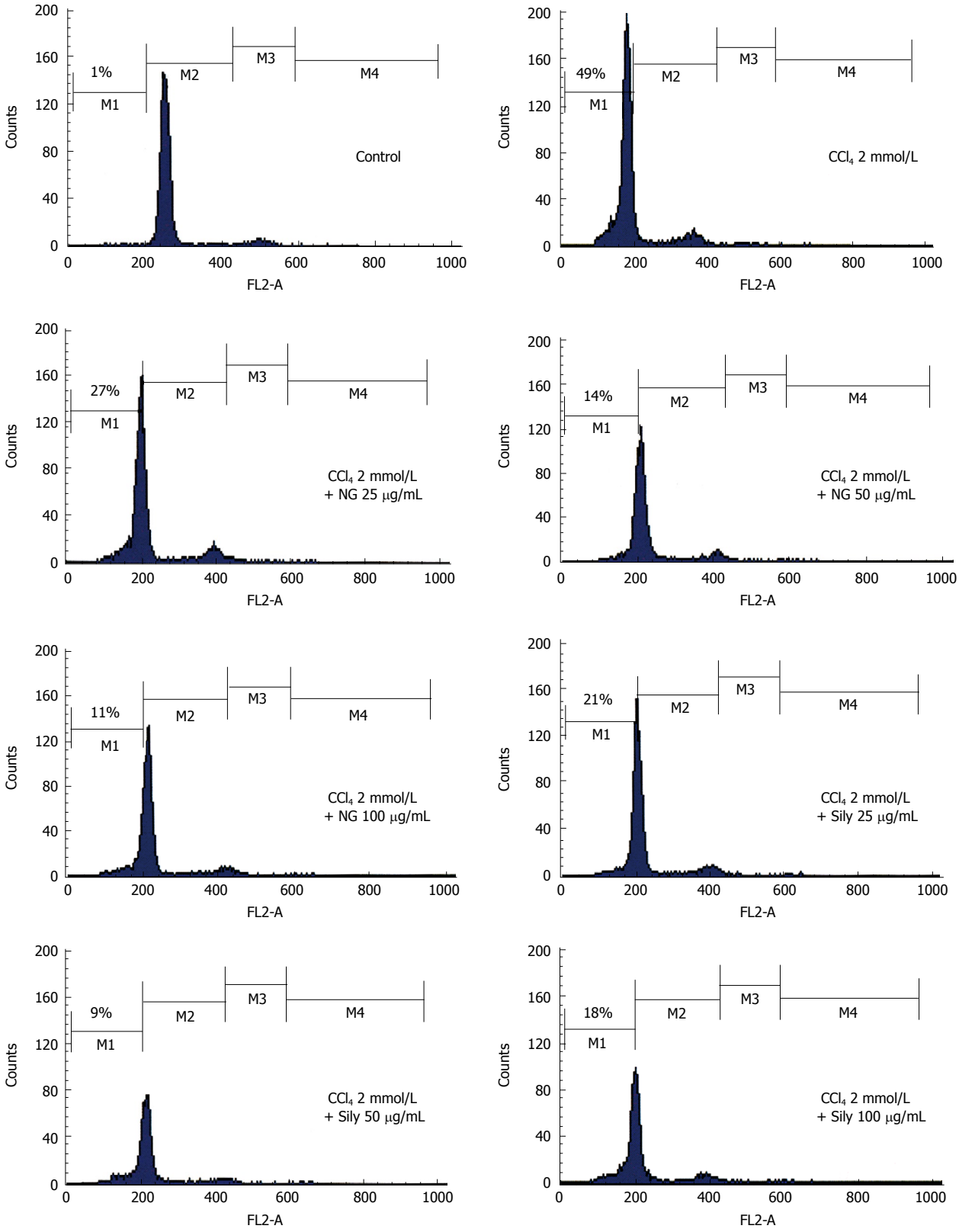

Figure 13 Effect of NG and silymarin against CCl_4-induced cell cycle arrest. HuH-7 cells were pre-incubated for 1 h with test materials (NG and silymarin) at mentioned concentrations. The cells were further incubated for 24 h with CCl_4 (2 mmol/L). Thereafter, cells were harvested by trypsinization, fixed with ethanol, stained with PI , and analyzed using flow cytometry. Representative histograms are shown, and the percentage of cells in the sub G_0/G_1 fraction (M1 zone, hypodiploid area) are shown.

Effect of NG and silymarin on CCl_4-induced depletion of GSH levels in HuH-7 cells

Figure 16 depicts the effect of CCl_4 on GSH levels and restorative effect of NG and silymarin in a dose-response manner. Treatment of HuH-7 cells with CCl_4-depleted the GSH content by 2 folds. Co-exposure with NG and silymarin effectively restored the depleted levels of GSH in a dose response manner. Restorative

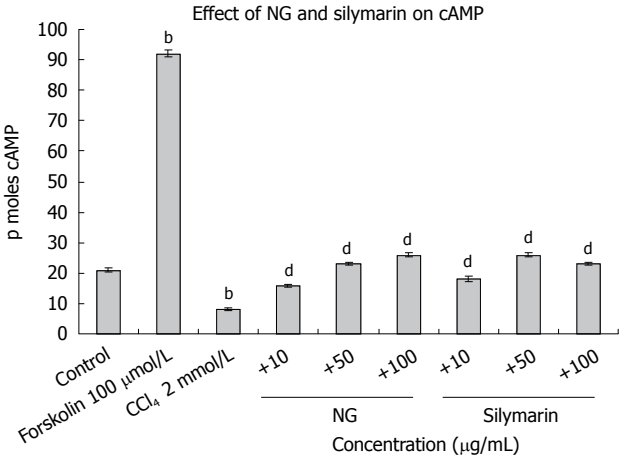

Figure 14 Effect of NG and silymarin against CCl_4-depleted cAMP levels. Pre-incubated, (1 hour at mentioned concentrations of NG and silymarin) HuH-7 cells were exposed to 2 mmol/L CCl_4 for 24 h. cAMP levels were determined in the cell culture supernatants as described in Materials and Methods. Forskolin (100 μmol/L) was used as positive control. Data are expressed as mean ± SD and are from representative experiments repeated twice and conducted in triplicate. Statistical significance: $^bP < 0.001$ *vs* the untreated control. $^dP < 0.001$ *vs* CCl_4-treated cells.

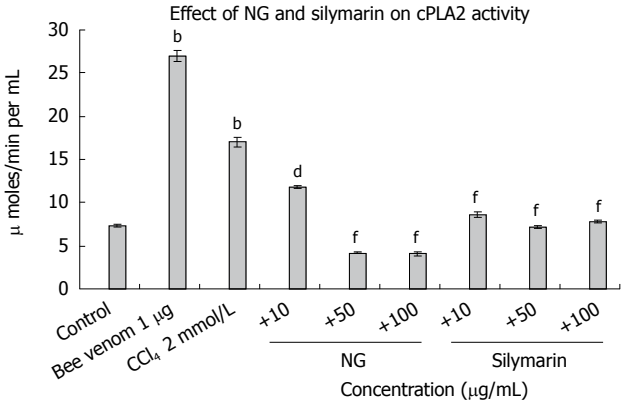

Figure 15 Effect of NG and silymarin against CCl_4-induced cPLA2 levels. Pre-incubated, (1 h with mentioned concentrations of NG and silymarin) HuH-7 cells were exposed to 2 mmol/L CCl_4 for 24 h. cPLA2 levels were determined as described in Materials and Methods. Bee venom (1 μg) was used as positive control. Data are expressed as mean ± SD and are from representative experiments repeated twice and conducted in triplicate. Statistical significance: $^bP < 0.001$ *vs* the untreated control; $^dP < 0.01$; $^fP < 0.001$ *vs* CCl_4-treated cells.

effect of NG was in the range of 17% to 147% at 5 mg/L to 100 mg/L, respectively. Silymarin showed an effect in the range of 23% to 152% at a concentration of 5 to 50 mg/L. However at higher concentration (100 mg/L), there was a slight decrease in this effect. BSO (100 μmol/L) was used as a positive inhibitor of GSH.

In vitro antioxidant activity of NG and silymarin

Figure 17 is representative of anti-oxidant activity of NG and silymarin. NG showed a strong activity, with I.C. 50 values of 17.31 mg/L for DPPH, 22.75 mg/L for enzymatic reaction, 13.49 mg/L for non-enzymatic reaction and 8.71 mg/L for ABTS assay. The IC 50 values of silymarin for the same assays were 34.07, 24.35, 21.10 and 12.36 mg/L respectively.

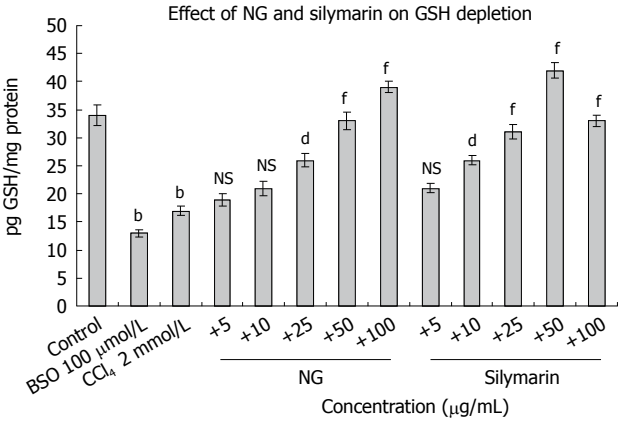

Figure 16 Effect of NG and silymarin on CCl_4-induced decrease in GSH levels. HuH-7 cells were pre-incubated with medium containing test materials (NG and silymarin) for 1 h. The cultures were then further incubated in presence and absence of CCl_4 for 24 h. The cells were harvested by scraping and GSH levels were determined as described under Materials and Methods section. BSO (100 μmol/L) was used as positive control. Data are expressed as mean ± SD and are from representative experiments repeated twice and conducted in triplicate. Statistical significance: $^bP < 0.001$ *vs* the untreated control; $^dP < 0.01$; $^fP < 0.001$; NS = non-significant *vs* CCl_4-treated cells.

DISCUSSION

Liver cells exposed to various chemicals/drugs (pro-oxidants) appear to be a useful *in vitro* model to characterize the biochemical and toxicological properties of such entities, and the possible protection provided by added agents[36]. The main goal of this work was to investigate the influence of an irridoid glycoside compound negundoside (NG) on CYP2E1-mediated toxicity in HuH-7 cells induced by CCl_4. Overall, the results of the present study indicate that NG is effective in protecting against the toxicity and the loss of viability induced by CCl_4.

The main mechanism by which CCl_4 is known to mediate its toxic effects is through oxidative stress and oxidative damage due to an increased production of ROS[37]. Induction of CYP2E1 by CCl_4 is one of the main pathways by which CCl_4 increases ROS production and generates a state of oxidative stress in the liver[38,39]. Since CYP2E1 is a key contributor to injury produced by CCl_4, one possible mechanism involved in the prevention of this toxicity by NG could have been an inhibition of CYP2E1 catalytic activity. Results in this study indicate that NG does not affect *p*-nitrophenol metabolism by CYP2E1 in liver microsomes under the experimental conditions (Figure 5 A and B); therefore, the mechanism by which NG affords its protection is not by inhibition of CYP2E1 activity. This is in confirmation to earlier reports in which many plant derived products like, *Scutellariae radix*[40], *Humulus lupulus*[41], green tea compounds[42] have also been shown to be hepatoprotective in other systems without any effect on CYP2E1 catalytic activity.

Bio-metals, such as iron are powerful catalysts of

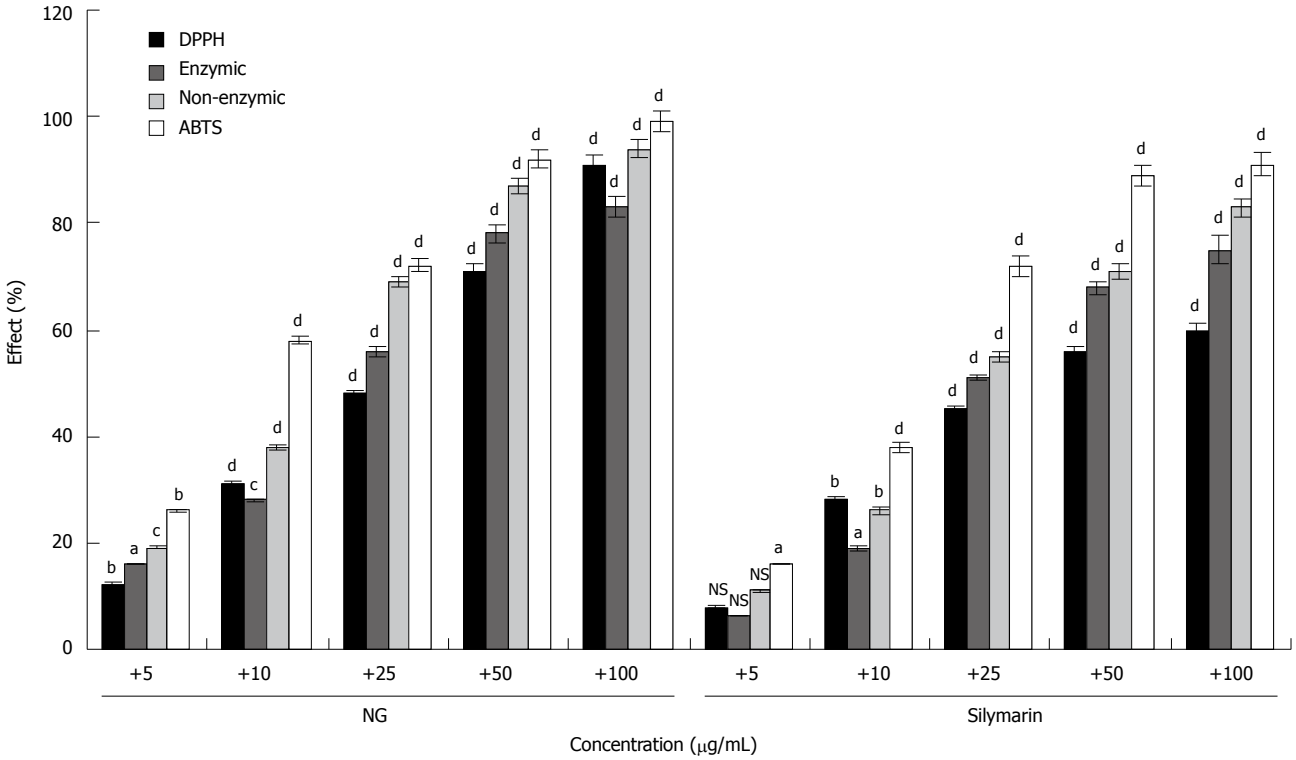

Figure 17 *In vitro* effect of NG and silymarin on free radicals generation. Free radicals scavenging effect of NG and silymarin was studied against DPPH radicals (stable hydroxyl radical), enzymic, non-enzymic (superoxide radicals) and ABTS radical (stable hydroxyl radical). Percentage anti-oxidant activity (% effect) was determined as described in Materials and Methods section. Values are mean from five independent determinations. $^{b}P < 0.001$ versus control. Control O.D. system DPPH, 0.650, system Enzymatic, 0.250 and system Non-enzymatic, 0.300 and system ABTS, 0.750. Data are expressed as mean ± SD and are from a representative experiments repeated twice and conducted in triplicate. Statistical significance: $^{a}P < 0.05$; $^{b}P < 0.01$; $^{c}P < 0.02$; $^{d}P < 0.001$; NS = non-significant *vs* respective controls.

free radical formation and lipid peroxidation processes, and polyunsaturated fatty acids in cellular membranes (microsomes) provide basic substrates for these reactions[43]. Scavenging or preventing formation of lipid radicals may prevent damage when cellular antioxidant defense mechanism is strengthened or iron overload is sequestered by exogenous treatment with cytoprotective drugs as NG. As lipid peroxidation (LPO) has been shown to play an important role in the ensuing toxicities in CYP2E1-induced conditions[44,45], in this respect, NG strongly inhibited lipid peroxidation promoted by H_2O_2+Fe in microsomes and CCl_4 in HuH-7 cells (Figure 6 A and B). It has been reported that glycosides, such as NG, are potent cytoprotective agents against oxidative stress induced cytotoxicity[46]. Therefore, one major mechanism underlying the effectiveness of NG in protecting against the CCl_4-induced LPO in HuH-7 cells may involve its capability to prevent lipid peroxidation chain reactions as a consequence of scavenging free radicals or chelating iron.

Intracellular calcium has been suggested to play a critical role in the oxidative damage of liver cells. Earlier, it has been reported that treatment of liver cells with CCl_4 increases calcium levels and produce cellular toxicity through calcium dependent pathways. Elevated levels of calcium initiates a cascade of signaling events leading to activation of calcium dependent degredative enzymes as phospholipases A2, endonucleases, or proteases[47]. Our results are in corroboration with this and showed that CCl_4-induced cell death in HuH-7 cells was mediated by release of intracellular calcium with subsequent activation of caspase 3 and cPLA2 (Figures 9 and 15) and simultaneous inhibition of cAMP levels (Figure 14). Increased intracellular calcium, activation of PLA2 and inhibition of cAMP were almost parallel to toxicity. Oxidative stress-mediated LPO is suggested to be the initiator of intracellular calcium release[25], which later influences down stream apoptotic signaling processes. cAMP levels are known to be regulated by catalytic activity of adenylate cyclase and phosphodiesterase. Increasing concentration of intracellular cAMP has been directly associated with inhibition of phosphodiesterase, reduced release of ROS and inhibition of chemotaxis, degranulation and cell death[48]. NG restored the calcium and cAMP to normal levels, inhibited lipid peroxidation, activated cPLA2 levels were inhibited and cytotoxicity was reversed without altering CYP2E1 levels. Therefore we hypothesize that NG inhibits CCl_4-induced oxidative stress and, hence LPO, which increases intracellular calcium and PLA2 activation and converge on mitochondria, inducing mitochondrial damage. All these downstream events of CYP2E1 mediated toxicity were effectively inhibited by NG, thus demonstrating its strong anti-oxidant capacity. We also suggest that inhibition of intracellular calcium release mediated cPLA2 activation, increase in cAMP levels, and restoration of MMP are the key factors in cytoprotection afforded by NG. Recently, it has been

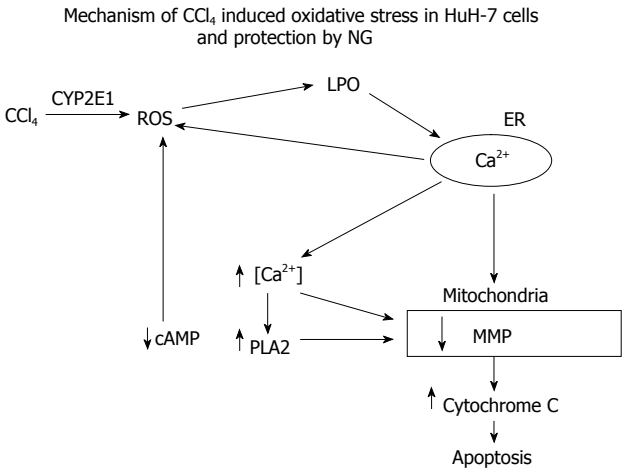

Figure 18 Proposed sequence of events and mechanism involved in the toxicity of CCl_4 and cytoprotection offered by NG. CCl_4 is activated by CYP 450 2E1 system and converted into trimethyl CCl_3 radicals inducing oxidative stress (increased ROS inducing membrane lipid peroxidation) and disturbed cellular Ca^{2+} homeostasis. Increase in intracellular Ca^{2+} concentrations leads to activation of phospholipase A2 and a decline in cAMP levels. All these signaling events converge onto the mitochondrial-initiating mitochondrial pore transition and ultimately to cellular injury. The highly increased levels of ROS is, in part, the consequence of the increase in Ca^{2+}, and also as a result of mitochondrial permeabilization resulting in activation of Ca^{2+} dependent proteases. NG exerts a protective effect *via* inhibition of oxidative stress, maintenance of disrupted intracellular calcium homeostasis and inactivation of Ca^{2+}-dependent proteases.

suggested that calcium levels do not play a direct role in toxicity[26], but that activation of PLA2, promotion of the mitochondrial permeability transition and loss of mitochondrial function, which are secondary manifestations of increased calcium levels, form a general pathway involved in the toxicity: all these events were restored to normal by NG.

As the main antioxidant inside mammalian cells, GSH plays a pivotal role in preventing oxidative stress and mitochondrial damage caused by numerous toxins[49]. Therefore, the effect of CCl_4 in the absence or presence of NG on GSH content was evaluated. CCl_4 treatment drastically depleted intracellular GSH in HuH-7 cells, an effect prevented in the presence of NG (Figure 16). Accordingly, the maintenance of intracellular GSH levels by NG may help in protecting against the oxidative toxicity induced by CCl_4 in HuH-7 cells and avoid cell degeneration and death. Previously as well, depletion of GSH has been shown to enhance CYP2E1 resulting in CYP2E1-derived ROS leading to toxicity[50].

Decreased MMP has been proposed to be a key mechanism by which CYP2E1-dependent LPO causes loss in cell viability. Mitochondria are a main source for generating ROS and, hence, a target for damage by oxidative stress[51]. In this respect, CCl_4 treatment caused a decrease in the MMP in HuH-7 cells, and this effect was prevented by NG as well as by silymarin (Figure 11). These results suggest that NG and silymarin may protect the cells by preventing oxidant-induced MMP transition leading to pathogenesis of necrotic or apoptotic cell death[52]. It has been proposed earlier that mitochondrial injury derived from oxidative damage can lead not only to necrosis by depleting ATP, but also to apoptotic cell death by inducing the release of mitochondrial factors such as cytochrome C, which activates the caspase cascade[53, 54].

Regardless of its precise mechanism of action, numerous studies in various animal models and in humans describe protective effects of NG against oxidative stress-related disease states[2-15]. This enhances its potential usefulness as a preventive agent toward oxidative damage involved in the development of liver injury caused by oxidative stress. Since NG acts as a very potent membrane stabilizer, it is also suggested that NG, may be acting as amphipathic substance, localizing near the membrane surface, trapping any radicals generated in the lipid environment of the membranes as well as in the cytosol. Such localization is suggested from the fact that CYP2E1 is found in the microsomes, and mitochondria appear to be a target for the CYP2E1-mediated damage in the presence of hepatotoxins such as CCl_4, which was effectively inhibited by NG. Moreover, NG is well tolerated without adverse health effects by humans even after oral administration at high doses as evident from its use in Asian traditional medicine practices for various ailments.

In conclusion, this report shows that NG can protect against CCl_4-induced toxicity and oxidative stress. The mechanism of protection involves decreased production of ROS and lipid peroxidation when the CYP2E1 mediated oxidative stress was produced in HuH-7 cells with pro-oxidant as CCl_4. The main mechanism involved in the cytoprotection of NG seems to be its ability to protect the mitochondria against depletion in its membrane potential, an event that is very critical in the loss of cell viability as a consequence of oxidative stress. This mechanism has been postulated in the Figure 18. NG has been shown to prevent CCl_4-induced liver injury, which may be, in part, due to the protection against CYP2E1-dependent oxidative stress as demonstrated in this study. NG supplementation could also prove to be protective against numerous toxicants that involve induction of oxidative stress through increased generation of ROS.

ACKNOWLEDGMENTS

We are grateful to Dr. GN Qazi, Director of this institute for providing constant guidance and support.

COMMENTS

Background

Vitex negundo is a reputed medicinal herb of Indian sub-continent. All plant parts are considered important in Ayurvedic system of medicine for various indications.

Research frontiers

Several pharmacological studies validate the medicinal claims of *Vitex negundo*. Diverse chemical constituents have been reported from various parts of this plant which are considered responsible for its varied pharmacological activities. The negundoside seems to be a potential constituent that exerts a protective effect on CYP2E1-dependent toxicity caused by carbon tetrachloride (CCl_4) *via* inhibition of lipid peroxidation, followed by an improved intracellular calcium homeostasis and inhibition of Ca^{2+}-dependent proteases.

Innovation and breakthrough

The present investigation shows that negundoside is a potent phytopharmaceutical that acts in a novel way in inhibiting liver toxicity by interfering in the key events that are the main causative factors leading to liver

dysfunction.

Applications

Negundoside exerts a protective action on CYP2E1-dependent oxidative stress and toxicity that may contribute to preventing chemically-induced liver injury, and may be useful in preventing toxicity by various other hepatotoxins as well.

Peer review

The authors investigated the anti-apoptotic effect of negundoside (NG), being extracted from leaves of Vitex negundo, on cultured human hepatoma cell line, HuH-7G2. The authors performed a large amount of experiments, and found that NG inhibited ROS formation, lipid peroxidation, intracellular calcium elevation, GSH depletion, elevated anti-oxidant activity, declined MMP, cytochrome C release, and finally carbon tetrachloride-medicated apoptosis. The manuscript addressed the authors' hypothesis with sufficient data.

REFERENCES

1 **Chin YW**, Balunas MJ, Chai HB, Kinghorn AD. Drug discovery from natural sources. *AAPS J* 2006; **8**: E239-E253

2 **Dharmasiri MG**, Jayakody JR, Galhena G, Liyanage SS, Ratnasooriya WD. Anti-inflammatory and analgesic activities of mature fresh leaves of Vitex negundo. *J Ethnopharmacol* 2003; **87**: 199-206

3 **Azhar-Ul-Haq**, Malik A, Khan MT, Anwar-Ul-Haq, Khan SB, Ahmad A, Choudhary MI. Tyrosinase inhibitory lignans from the methanol extract of the roots of Vitex negundo Linn. and their structure-activity relationship. *Phytomedicine* 2006; **13**: 255-260

4 **Jagetia GC**, Baliga MS. The evaluation of nitric oxide scavenging activity of certain Indian medicinal plants in vitro: a preliminary study. *J Med Food* 2004; **7**: 343-348

5 **Alam MI**, Gomes A. Snake venom neutralization by Indian medicinal plants (Vitex negundo and Emblica officinalis) root extracts. *J Ethnopharmacol* 2003; **86**: 75-80

6 **Chandramu C**, Manohar RD, Krupadanam DG, Dashavantha RV. Isolation, characterization and biological activity of betulinic acid and ursolic acid from Vitex negundo L. *Phytother Res* 2003; **17**: 129-134

7 **J Munasinghe TC**, Seneviratne CK, Thabrew MI, Abeysekera AM. Antiradical and antilipoperoxidative effects of some plant extracts used by Sri Lankan traditional medical practitioners for cardioprotection. *Phytother Res* 2001; **15**: 519-523

8 **Gupta M**, Mazumder UK, Bhawal SR. CNS activity of Vitex negundo Linn. in mice. *Indian J Exp Biol* 1999; **37**: 143-146

9 **Avadhoot Y**, Rana AC. Hepatoprotective effect of Vitex negundo against carbon tetrachloride-induced liver damage. *Arch Pharm Res* 1991; **14**: 96-98

10 **Perumal Samy R**, Ignacimuthu S, Sen A. Screening of 34 Indian medicinal plants for antibacterial properties. *J Ethnopharmacol* 1998; **62**: 173-1782

11 **Damayanti M**, Susheela K, Sharma GJ. Effect of plant extracts and systemic fungicide on the pineapple fruit-rotting fungus, Ceratocystis paradoxa. *Cytobios* 1996; **86**: 155-165

12 **Pushpalatha E**, Muthukrishnan J. Larvicidal activity of a few plant extracts against Culex quinquefasciatus and Anopheles stephensi. *Indian J Malariol* 1995; **32**: 14-23

13 **Bhargava SK**. Antiandrogenic effects of a flavonoid-rich fraction of Vitex negundo seeds: a histological and biochemical study in dogs. *J Ethnopharmacol* 1989; **27**: 327-339

14 **Hebbalkar DS**, Hebbalkar GD, Sharma RN, Joshi VS, Bhat VS. Mosquito repellent activity of oils from Vitex negundo Linn. leaves. *Indian J Med Res* 1992; **95**: 200-203

15 **Prabhakar A**, Gupta BD, Suri KA, Satti NK, Malhotra S, Gupta KK, Sharma VK, Johri RK, Jaggi BS, Chandan BK, Shankar L, Bedi KL, Suri OP, Qazi GN. Hepatoprotective activity of 2'-p-hydroxybenzoylmussaenodidic acid. United States patent, US Patent 7, 259, 148, 2007; **259:** 148

16 **Dey A**, Caro AA, Cederbaum AI. S-adenosyl methionine protects ob/ob mice from CYP2E1-mediated liver injury. *Am J Physiol Gastrointest Liver Physiol* 2007; **293**: G91-G103

17 **Kume Y**, Ikeda H, Inoue M, Tejima K, Tomiya T, Nishikawa T, Watanabe N, Ichikawa T, Kaneko M, Okubo S, Yokota H, Omata M, Fujiwara K, Yatomi Y. Hepatic stellate cell damage may lead to decreased plasma ADAMTS13 activity in rats. *FEBS Lett* 2007; **581**: 1631-1634

18 **Beddowes EJ**, Faux SP, Chipman JK. Chloroform, carbon tetrachloride and glutathione depletion induce secondary genotoxicity in liver cells via oxidative stress. *Toxicology* 2003; **187**: 101-115

19 **Jimenez-Lopez JM**, Cederbaum AI. Green tea polyphenol epigallocatechin-3-gallate protects HepG2 cells against CYP2E1-dependent toxicity. *Free Radic Biol Med* 2004; **36**: 359-370

20 **Lee CS**, Kim YJ, Han ES. Glycyrrhizin protection against 3-morpholinosydnonime-induced mitochondrial dysfunction and cell death in lung epithelial cells. *Life Sci* 2007; **80**: 1759-1767

21 **Gandhidasan R**, Thamaraichelvan, Baburaj S. Anti inflammatory action of Lannea coromandelica by HRBC membrane stabilization. *Fitoterapia* 1991; **62**: 81-83

22 **Tasduq SA**, Kaiser P, Sharma SC, Johri RK. Potentiation of isoniazid-induced liver toxicity by rifampicin in a combinational therapy of antitubercular drugs (rifampicin, isoniazid and pyrazinamide) in Wistar rats: A toxicity profile study. *Hepatol Res* 2007; **37**: 845-853

23 **Tietze F**. Enzymic method for quantitative determination of nanogram amounts of total and oxidized glutathione: applications to mammalian blood and other tissues. *Anal Biochem* 1969; **27**: 502-522

24 **Nakagawa Y**, Suzuki T, Kamimura H, Nagai F. Role of mitochondrial membrane permeability transition in N-nitrosofenfluramine-induced cell injury in rat hepatocytes. *Eur J Pharmacol* 2006; **529**: 33-39

25 **Kawamura-Sato K**, Hirama Y, Agata N, Ito H, Torii K, Takeno A, Hasegawa T, Shimomura Y, Ohta M. Quantitative analysis of cereulide, an emetic toxin of Bacillus cereus, by using rat liver mitochondria. *Microbiol Immunol* 2005; **49**: 25-30

26 **Caro AA**, Cederbaum AI. Role of intracellular calcium and phospholipase A2 in arachidonic acid-induced toxicity in liver cells overexpressing CYP2E1. *Arch Biochem Biophys* 2007; **457**: 252-263

27 **Rameh LE**, Rhee SG, Spokes K, Kazlauskas A, Cantley LC, Cantley LG. Phosphoinositide 3-kinase regulates phospholipase Cgamma-mediated calcium signaling. *J Biol Chem* 1998; **273**: 23750-23757

28 **Grynkiewicz G**, Poenie M, Tsien RY. A new generation of Ca2+ indicators with greatly improved fluorescence properties. *J Biol Chem* 1985; **260**: 3440-3450

29 **Caro AA**, Cederbaum AI. Ca2+-dependent and independent mitochondrial damage in HepG2 cells that overexpress CYP2E1. *Arch Biochem Biophys* 2002; **408**: 162-170

30 **Emaus RK**, Grunwald R, Lemasters JJ. Rhodamine 123 as a probe of transmembrane potential in isolated rat-liver mitochondria: spectral and metabolic properties. *Biochim Biophys Acta* 1986; **850**: 436-448

31 **Rothe G**, Valet G. Flow cytometric analysis of respiratory burst activity in phagocytes with hydroethidine and 2',7'-dic hlorofluorescin. *J Leukoc Biol* 1990; **47**: 440-448

32 **Katiyar SK**, Afaq F, Azizuddin K, Mukhtar H. Inhibition of UVB-induced oxidative stress-mediated phosphorylation of mitogen-activated protein kinase signaling pathways in cultured human epidermal keratinocytes by green tea polyphenol (-)-epigallocatechin-3-gallate. *Toxicol Appl Pharmacol* 2001; **176**: 110-117

33 **Yang D**, Yaguchi T, Yamamoto H, Nishizaki T. Intracellularly transported adenosine induces apoptosis in HuH-7 human hepatoma cells by downregulating c-FLIP expression causing caspase-3/-8 activation. *Biochem Pharmacol* 2007; **73**: 1665-1675

34 **Gonzalez-Avila M**, Arriaga-Alba M, de la Garza M, del

Carmen HernandezPretelin M, Dominguez-Ortiz MA, Fattel-Fazenda S, Villa-Trevino S. Antigenotoxic, antimutagenic and ROS scavenging activities of a Rhoeo discolor ethanolic crude extract. *Toxicol In Vitro* 2003; **17**: 77-83

35 **Tasduq SA**, Kaisar P, Gupta DK, Kapahi BK, Maheshwari HS, Jyotsna S, Johri RK. Protective effect of a 50% hydroalcoholic fruit extract of Emblica officinalis against anti-tuberculosis drugs induced liver toxicity. *Phytother Res* 2005; **19**: 193-197

36 **Cao J**, Jiang LP, Liu Y, Yang G, Yao XF, Zhong LF. Curcumin-induced genotoxicity and antigenotoxicity in HepG2 cells. *Toxicon* 2007; **49**: 1219-1222

37 **Arteel GE**. Oxidants and antioxidants in alcohol-induced liver disease. *Gastroenterology* 2003; **124**: 778-790

38 **Morimoto M**, Hagbjork AL, Nanji AA, Ingelman-Sundberg M, Lindros KO, Fu PC, Albano E, French SW. Role of cytochrome P4502E1 in alcoholic liver disease pathogenesis. *Alcohol* 1993; **10**: 459-464

39 **Tsukamoto H**. Cyp2e1 and ALD. *Hepatology* 2000; **32**: 154-156

40 **Kim JY**, Lee S, Kim DH, Kim BR, Park R, Lee BM. Effects of flavonoids isolated from Scutellariae radix on cytochrome P-450 activities in human liver microsomes. *J Toxicol Environ Health A* 2002; **65**: 373-381

41 **Henderson MC**, Miranda CL, Stevens JF, Deinzer ML, Buhler DR. In vitro inhibition of human P450 enzymes by prenylated flavonoids from hops, Humulus lupulus. *Xenobiotica* 2000; **30**: 235-251

42 **Obermeier MT**, White RE, Yang CS. Effects of bioflavonoids on hepatic P450 activities. *Xenobiotica* 1995; **25**: 575-584

43 **Wilhelm J**. Metabolic aspects of membrane lipid peroxidation. *Acta Univ Carol Med Monogr* 1990; **137**: 1-53

44 **Caro AA**, Cederbaum AI. Synergistic toxicity of iron and arachidonic acid in HepG2 cells overexpressing CYP2E1. *Mol Pharmacol* 2001; **60**: 742-752

45 **Chen Q**, Galleano M, Cederbaum AI. Cytotoxicity and apoptosis produced by arachidonic acid in Hep G2 cells overexpressing human cytochrome P4502E1. *J Biol Chem* 1997; **272**: 14532-14541

46 **Moon MK**, Choi BM, Oh GS, Pae HO, Kim JD, Oh H, Oh CS, Kim DH, Rho YD, Shin MK, Lee HS, Chung HT. Catalposide protects Neuro 2A cells from hydrogen peroxide-induced cytotoxicity via the expression of heme oxygenase-1. *Toxicol Lett* 2003; **145**: 46-54

47 **Manibusan MK**, Odin M, Eastmond DA. Postulated carbon tetrachloride mode of action: a review. *J Environ Sci Health C Environ Carcinog Ecotoxicol Rev* 2007; **25**: 185-209

48 **Matsuhashi T**, Otaka M, Odashima M, Jin M, Komatsu K, Konishi N, Wada I, Sato T, Horikawa Y, Ohba R, Oyake J, Hatakeyama N, Watanabe S. Specific type IV phosphodiesterase inhibitor ameliorates thioacetamide-induced liver injury in rats. *J Gastroenterol Hepatol* 2005; **20**: 135-140

49 **Balasubramaniyan V**, Shukla R, Murugaiyan G, Bhonde RR, Nalini N. Mouse recombinant leptin protects human hepatoma HepG2 against apoptosis, TNF-alpha response and oxidative stress induced by the hepatotoxin-ethanol. *Biochim Biophys Acta* 2007; **1770**: 1136-1144

50 **Zhuge J**, Cederbaum AI. Depletion of S-adenosyl-l-methionine with cycloleucine potentiates cytochrome P450 2E1 toxicity in primary rat hepatocytes. *Arch Biochem Biophys* 2007; **466**: 177-185

51 **Wu D**, Cederbaum AI. Cyclosporine A protects against arachidonic acid toxicity in rat hepatocytes: role of CYP2E1 and mitochondria. *Hepatology* 2002; **35**: 1420-1430

52 **Lemasters JJ**, Nieminen AL, Qian T, Trost LC, Elmore SP, Nishimura Y, Crowe RA, Cascio WE, Bradham CA, Brenner DA, Herman B. The mitochondrial permeability transition in cell death: a common mechanism in necrosis, apoptosis and autophagy. *Biochim Biophys Acta* 1998; **1366**: 177-196

53 **Lemasters JJ**, Qian T, Bradham CA, Brenner DA, Cascio WE, Trost LC, Nishimura Y, Nieminen AL, Herman B. Mitochondrial dysfunction in the pathogenesis of necrotic and apoptotic cell death. *J Bioenerg Biomembr* 1999; **31**: 305-319

54 **Hoek JB**, Cahill A, Pastorino JG. Alcohol and mitochondria: a dysfunctional relationship. *Gastroenterology* 2002; **122**: 2049-2063

S- Editor Yang RH **L- Editor** Negro F **E- Editor** Ma WH